

## Final Report

**Federal Agency and Organization:** DOE EERE – Geothermal Technologies Program

**Recipient Organization:** Energy & Geoscience Institute (EGI), University of Utah

**DUNS Number:** 009095365

**Recipient Address:** 423 Wakara Way suite 300, Salt Lake City, Utah 84108

**Award Number:** DE-EE0007604

**Project Title:** Western USA Assessment of High Value Materials in Geothermal Fluids and Produced Fluids

**Project Period:** July 1, 2016 to December 31, 2018

**Principal Investigator:** Stuart Simmons  
Research Professor  
ssimmons@egi.utah.edu  
801-581-4122

**Date of Report Submission:** March 18, 2019

**Reporting Period:** July 1, 2016 to December 31, 2018

**Project Partners:** Utah Geological Survey (cost share partner)  
1594 W. North Temple St., Salt Lake City, UT 84114

US Geological Survey  
Central Mineral and Environmental Resources Science Center  
Box 25046, MS-973, Denver Federal Center, Denver, CO 80225

Signature  Date 3-18-2019

\*The Prime Recipient certifies that the information provided in this report is accurate and complete as of the date shown.

This report is written for public disclosure.

## EXECUTIVE SUMMARY

This report documents the results of investigations dealing with the concentrations and availabilities of strategic, critical and valuable materials (SCVM) in produced waters from geothermal and hydrocarbon reservoirs (50-250° C) in Idaho, Nevada, New Mexico, Oregon, and Utah. Analytical results were obtained for water samples from 47 production wells in 12 geothermal fields. Results were also obtained for samples from 25 oil/gas production wells in the Uinta and Paradox Basins and Covenant oil field, from 14 groundwater wells in the Tularosa play fairway (New Mexico), and from 20 groundwater wells and hot springs in the Sevier Thermal Belt (southwestern Utah).

Most SCVM concentrations in produced waters range from <0.1 to 100 ug/kg. Lithium is the only element, which has much higher concentrations and which ranges from 10 to 26,000 ug/kg. Relatively high concentrations of gallium (10-80 ug/kg geothermal; 10-10,000 ug/kg Uinta Basin), germanium (1-70 ug/kg geothermal; 10-500 ug/kg Uinta and Paradox Basins), scandium (0.1-2.0 ug/kg geothermal; 5-10 ug/kg Paradox Basin), selenium (1-100 ug/kg geothermal; 10-20,000 ug/kg Uinta and Paradox Basins), and tellurium (0.1-10 ug/kg geothermal; 1-500 ug/kg Uinta and Paradox Basins) are measured too. Geothermal production waters contain very low concentrations of REEs, below analytical detections limits of 0.01 ug/kg, but the concentrations of some REEs (lanthanum, cerium, and europium) range from 0.05 to 5 ug/kg in Uinta Basin waters.

Among the geothermal fields, the Roosevelt Hot Spring reservoir appears to have the largest endowments of germanium (20,000 kg) and lithium (7 million kg), the Patua reservoir appears to have the largest endowments of gallium (25,000 kg), selenium (47,000 kg), and tellurium (2500 kg), and the Raft River reservoir appears to have the large endowment of scandium (700 kg). By comparison, the Uinta Basin has larger inventories of gallium (>100,000 kg). These estimates are provisional, and they were calculated using geologically reasonable values for reservoir volumes and porosities.

The concentrations of gallium, germanium, lithium, scandium, selenium, and tellurium in produced waters appear to be partly controlled by reservoir temperature and concentrations of total dissolved salts. The relatively high concentration and large endowment of lithium occurring at Roosevelt Hot Springs appears to be related to hot water interaction with crystalline granitic rocks, which host the reservoir and the hydrothermal system, and elevated concentrations of TDS. Analyses of calcite scales from Dixie Valley show that cobalt, gallium, gold, palladium, selenium and tellurium are depositing at deep levels in production wells due to boiling. Comparisons with SCVM mineral deposits suggest that brines in sedimentary basins or derived from lacustrine evaporites enable aqueous transport of gallium, germanium, and lithium.

## BACKGROUND

This project deals with resource assessment of strategic, critical and valuable materials (SCVM), in production fluids and reservoirs across several western states (Idaho, Nevada, New Mexico, Oregon, and Utah). SCVM comprise a wide range of diverse elements, including alkali metals

This report is written for public disclosure.

(Li), noble gases (He,  $^3\text{He}$ ), metals and metalloids (Ag, Co, Ga, Ge, In, Ir, Nb, Os, Pd, Pt, Re, Rh, Ru, Se, Te), and rare earth elements (REEs: Ce, Dy, Er, Eu, Gd, Ho, La, Lu, Pr, Nd, Sc, Sm, Tb, Tm, Y, Yb)(e.g., Critical Metals Strategy, DoE, 2011; Energy Critical Elements, American Physical Society and Materials Research Society, 2011). This work contributes fundamental understanding to a US-wide resource assessment of the availability of SCVM in produced waters, especially those associated with geothermal fields that are currently utilizing hot water supply for direct use and electricity generation. This work supports a multi-year effort by DOE to enhance value streams for geothermal energy development.

The results and achievements described below are the products of a project spanning two years that were primarily focused on sampling and analyzing waters, plus some gases, from a large number of geothermal wells and hot springs associated with hydrothermal activity in the Basin and Range geologic province (Figs. 1-6). Produced waters were also sampled and analyzed from oil and gas wells in the Uinta basin, the Paradox basin, and the Covenant oil field. These data represent water compositions derived from geothermal and hydrocarbon reservoirs, ranging from 50-250° C. Supporting analytical data were obtained for rock samples, mainly drill cuttings but also from a few outcrops, associated with produced water sample sites. The first order interpretations of these data are focused on quantifying the concentrations of SCVM in produced waters and the inventories of SCVM in associated subsurface reservoirs. Effort is also directed at resolving geologic and geochemical controls on the supply and concentrations of SCVM.

Basin and Range geothermal resources were targeted for this study for three main reasons:

- they are generally associated with small scale, intermediate temperature reservoirs that could potentially benefit from enhanced value streams;
- they occur in a region that has considerable exploration potential for discovery of new geothermal resources (e.g. Coolbaugh et al., 2005; Williams et al., 2008; Allis et al., 2011; Blackwell et al., 2011)
- field operators (AltaRock, Cyrq, US Department of Defense, Elk Resources, Milgro, Newfield, PacifiCorp, QEP, TerraGen, and US Geothermal) were receptive and helpful with direct sampling of fluids from production wells.

The Basin and Range province as referred to in this report follows the definition of Eaton (1982) and Dickinson (2006). It is characterized by anomalously high regional heat flow related to tectonic extension, and it incorporates a number of geothermal fields within a very large region (Lachenbruch and Sass, 1978; Coolbaugh et al., 2005; Blackwell et al., 2011). Hydrothermal activity (as represented by hot springs and the locations of producing geothermal fields) is commonly associated with active fault systems resulting from regional extension that are situated near or along range fronts and basin margins. (e.g., Benoit and Butler 1983; Elders and Moore, 2016). These fault systems provide pathways for deep hot water circulation and convective heat transfer (e.g., Sorey et al., 1982; Faulds and Hinz, 2015; Person et al., 2008). There is also evidence of potential geothermal resources associated with hot sedimentary aquifers (e.g., Allis et al, 2011, 2015; Simmons et al., 2017), which are of interest because they potentially contain large volumes of hot metal-bearing fluid in laterally extensive sedimentary rock formations. Although EGS-type resources exist in hot low permeability rocks (e.g., Benato et al., 2016;

This report is written for public disclosure.

Bradford et al. 2016; Moore et al., 2019), these were not studied because they remain undeveloped and significant volumes of geothermal fluid have yet to be produced. The geological settings of each of the production fields studied are summarized in Table 1.

The main outcomes of this work that are covered in detail below comprise:

- Tabulations of concentrations and estimated inventories of SCVM in produced waters from geothermal fields in Idaho, Nevada, New Mexico, Oregon, and Utah.
- Tabulations of concentrations and estimated inventories of SCVM in produced waters oil/gas fields in eastern Utah.
- A preliminary assessment of the potential processes that control hydrothermal transport of SCVM, based on a regional study of the Sevier Thermal Belt.
- A comparative analysis of geologic settings of SCVM in modern production fluids and nearby mineral deposits.

The datasets are compiled into tables as Excel worksheets. These are supplied as separate files, and they represent integral components of this report:

- Table 1. Field Characteristics summarizes information regarding production, wells, geology, temperature, and reservoir volumes of the fields studied.
- Table 2. Geochemistry of Produced Fluids Idaho, Nevada, New Mexico, Oregon, and Utah contains field sample locations, analytical methods, and a comprehensive geochemical characterization of the fluid samples, including the concentrations of SCVM in produced waters, and first order estimates of SCVM inventories. Data and methods are presented in 17 worksheets: Introduction; Beowawe, NV; Blue Mountain, NV; Dixie Valley, NV; Lightning Dock, NM; Neals Hot Spring, OR; Newcastle, UT; North Milford valley, UT; Paradox Basin, UT; Patua, NV; Raft River, ID; Roosevelt Hot Springs, UT; San Emidio, NV; Sevier thermal belt, UT; Soda Lake, NV; Thermo, UT; Tularosa, NM; Uinta Basin, UT; Field-Sample Blanks for QC (quality control).
- Table 3. Geochemistry of Reservoir Rocks, and Calcite Scales, Nevada-Utah contains trace element and SCVM concentrations in rock samples made of drill cuttings from production wells in three geothermal fields (Beowawe, Dixie Valley, Roosevelt Hot Springs), drill cuttings from production wells in the Uinta and Paradox Basins, and from surface outcrops in the Sevier Thermal Belt. Data and methods are divided between seven worksheets: Introduction; Beowawe, NV; Dixie Valley, NV; Dixie Valley Calcite Scales; Paradox Basin, UT; Roosevelt Hot Springs, UT; Sevier Thermal Belt, UT; Uinta Basin, UT.
- Table 4. Lithology and Mineralogy of Drill Cuttings from Beowawe, Dixie Valley and Roosevelt Hot Springs contains mineralogical and lithological data for rock samples from geothermal wells at Beowawe, Dixie Valley, and Roosevelt Hot Springs that have been geochemically analyzed for SCVM (Table 3).
- Table 5. Geological Settings of Critical Metal Mineral Deposits summarizes the geological

This report is written for public disclosure.

settings and characteristics of SCVM ore deposits. The attributes are compiled in eleven separate worksheets: Introduction; Cobalt; Gallium; Germanium; Indium; Lithium; Niobium; Platinum Group Elements; REE; Rhenium; Scandium; Selenium; Tellurium.

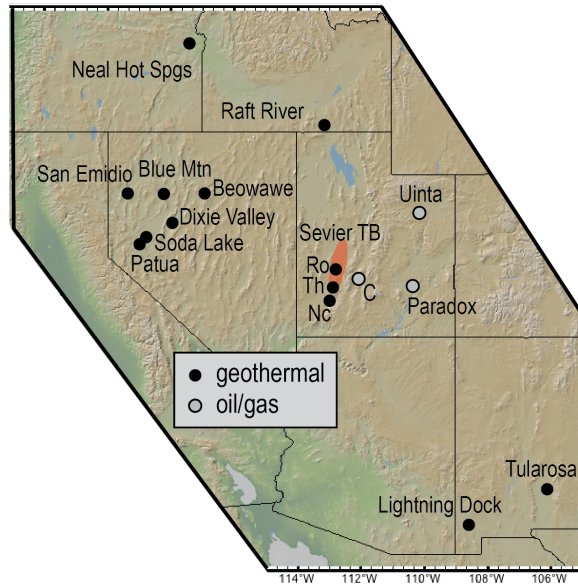


Figure 1. Production fluid sampling sites. Abbreviations: C=Covenant; Nc=Newcastle; Ro=Roosevelt Hot Springs; Sevier TB=Sevier thermal belt (orange); Th=Thermo. Base map is from Ryan et al (2009).

## FLUID SAMPLING METHODS

Water samples were collected from all study sites, including hot springs and production wells, whereas gas samples were collected from a small subset of sites. These gas samples are of two types, one is for analyzing helium and helium isotopes (Beowawe, Neal Hot Springs, North Milford Valley Paradox Basin, Patua, Raft River, San Emidio, Sevier Thermal Belt, Soda Lake, and Uinta Basin), and the other is for analyzing gases in steam where produced fluids are two-phase at the wellhead (Beowawe, Dixie Valley, Roosevelt Hot Springs-Blundell). Details of how fluid samples were acquired and treated are described below.

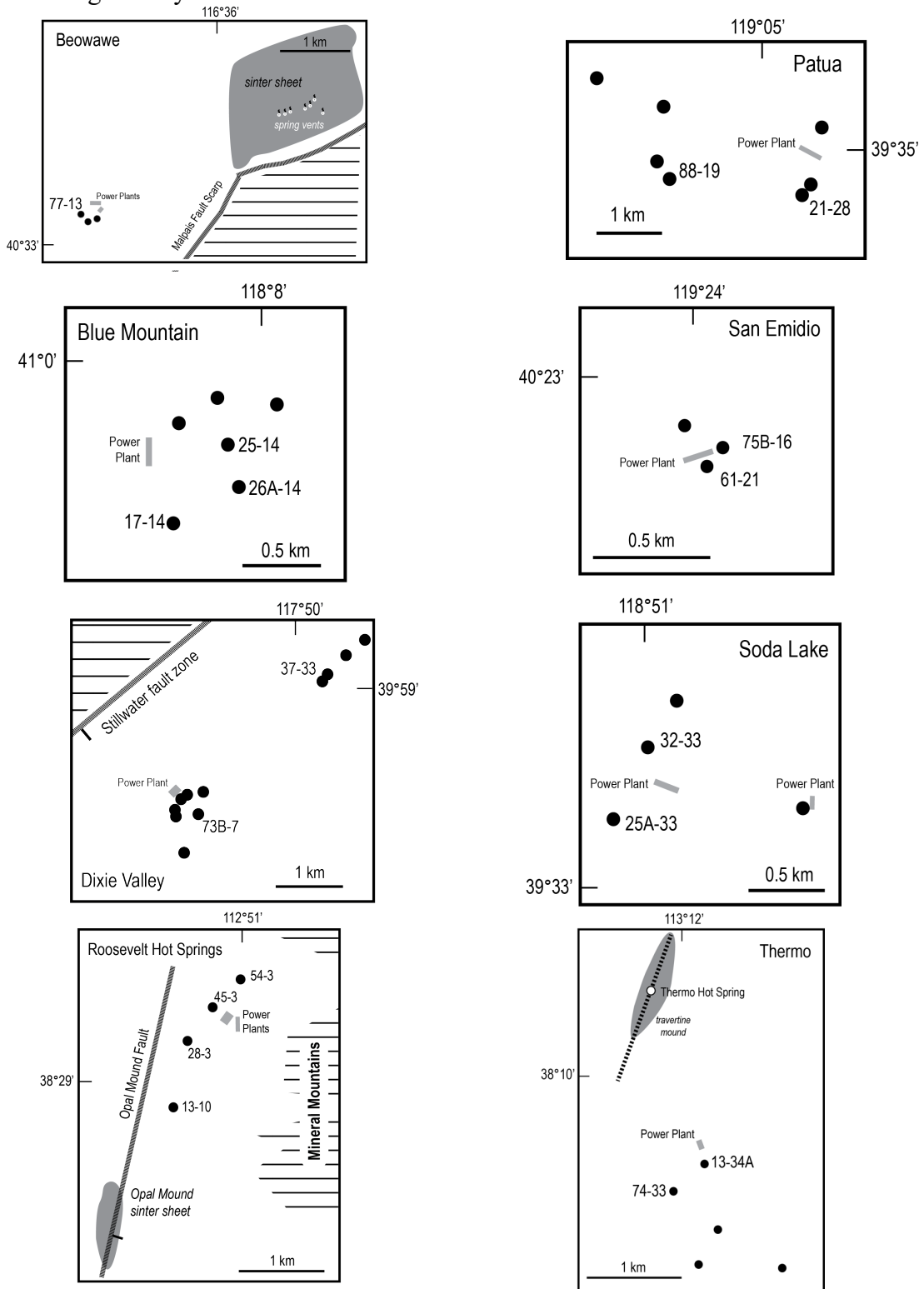
### *Geothermal production wells*

The methodology for acquiring fluid samples from geothermal wells depends on several factors, including the location(s) and availability of pipeline sample ports and temperature and pressure conditions.

Where the wells are pumped to produce geothermal fluid (Blue Mountain, Lightning Dock, Neal Hot Springs, Newcastle, Patua, Raft River, San Emidio, Soda Lake, Thermo), pipelines are filled with hot single-phase liquid that flows under pressure, and samples were acquired with stainless

This report is written for public disclosure.

steel coiled tubing submerged in an ice bath to prevent gas phase separation. Sample ports on pipelines are generally located within 10-20 m of the wellhead.



This report is written for public disclosure.

Figure 2. Sketch maps of geothermal production fields and wells sampled for waters in Nevada and Utah.

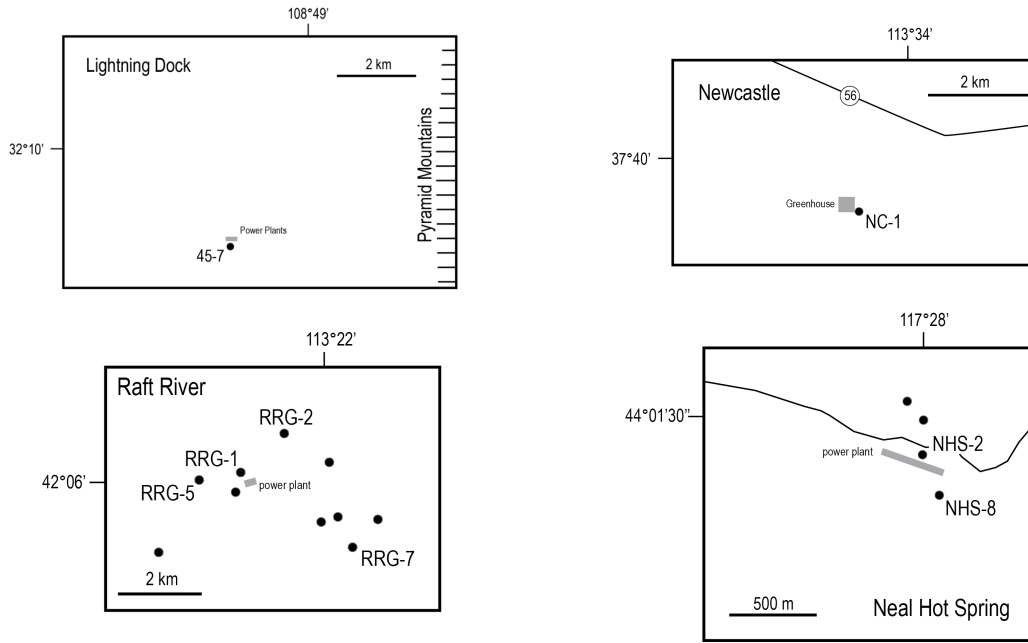


Figure 3. Sketch maps of geothermal production fields and wells sampled for waters in Idaho, New Mexico, Oregon and Utah.

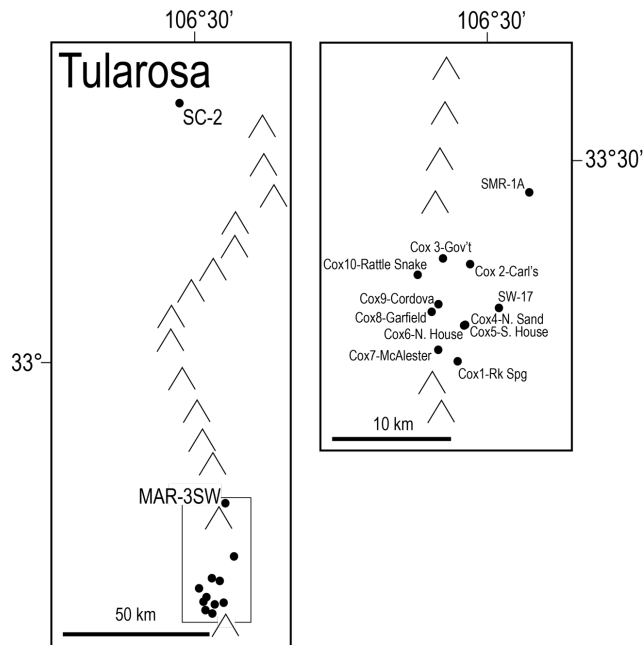


Figure 4. Sketch map of the groundwater wells sampled at the Tularosa geothermal prospect, New Mexico.

This report is written for public disclosure.

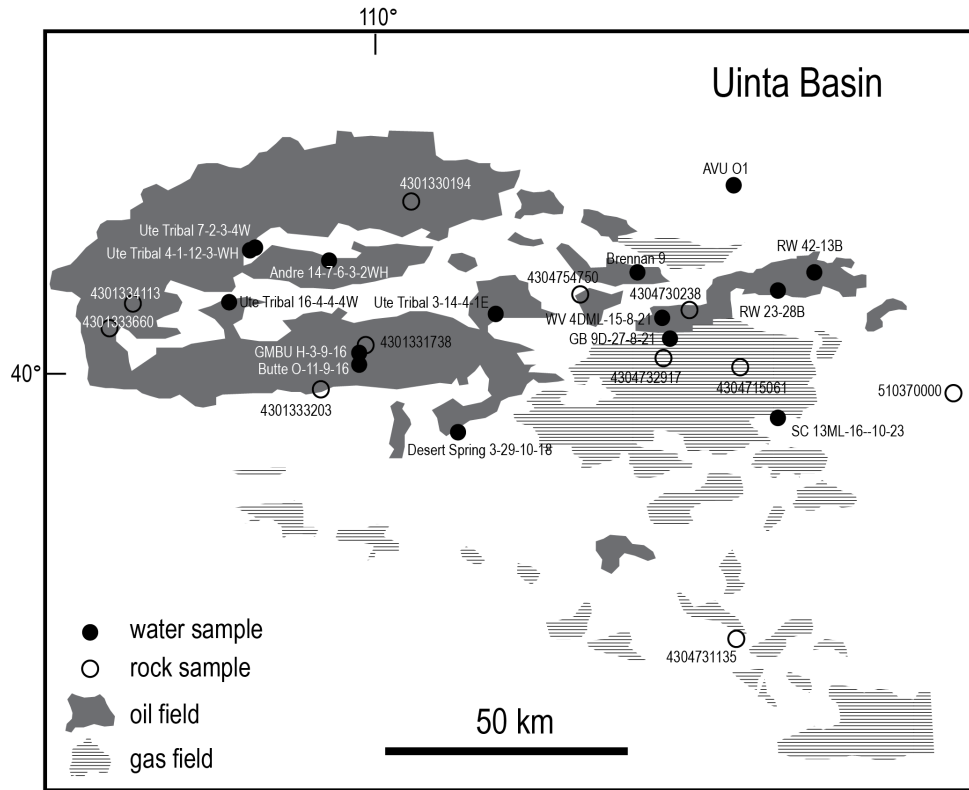


Figure 5. Sketch map of the Uinta Basin showing the oil and gas wells sampled for waters and drill cuttings.

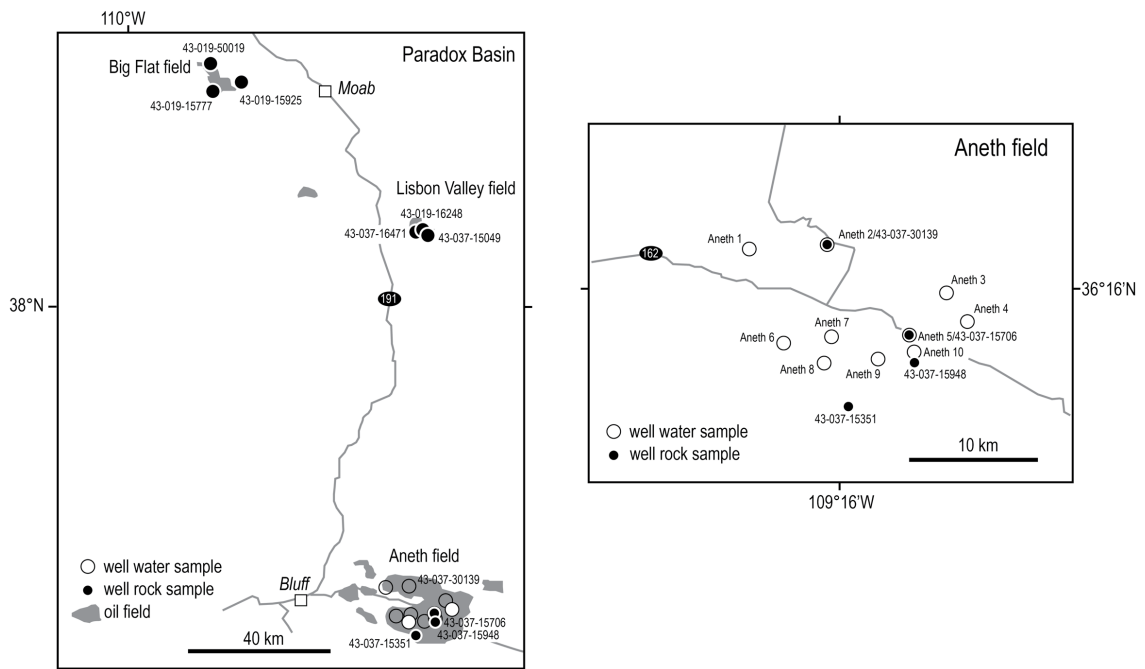


Figure 6. Sketch map of the Paradox Basin showing the oil wells sampled for waters and drill cuttings.

This report is written for public disclosure.

Where the wells are self-flowing and fluid production is two-phase, comprising liquid and steam (Beowawe, Dixie Valley and Roosevelt Hot Springs), a mini-separator is attached to the pipeline to collect separate water and gas samples (Fig. 7A). During collection of either the water or the gas sample, the fluid is run through stainless steel coiled tubing submerged in an ice bath. The water sample is collected into an open beaker. At Dixie Valley and Roosevelt Hot Springs-Blundell, some wells also have drip tanks (Fig. 7B), where separated water is conductively cooled and these were sampled too.

At Thermo, the wells are pumped, but the mini-separator (described below) was utilized to collect a sample, which provided the opportunity to acquire both water and gas samples.

Gas samples were collected from four fields (Beowawe, Dixie Valley, Roosevelt Hot Springs, and Thermo), using the mini-separator and stainless-steel coiled tubing submerged in an ice bath. The resulting mixture of water and gas was collected into an evacuated glass bulb that is partially filled with caustic soda (4N NaOH). Early on we discovered some issues with leakage from sample bottles, and repeat sampling was undertaken to ensure high quality samples were analyzed.

Helium and helium isotope samples were collected by filling a long copper tube with water (no gas bubbles) from the stainless-steel coil submerged in an ice bath. The water sample is untreated, and the ends of the copper tube are clamped to form the seal.

A.



B.



Figure 7. Fluid sampling sites, Roosevelt Hot Springs: A) mini-separator on a two-phase line, upstream of the separator, with steam jetting from the gas port; B) pipeline downstream of a separator with a drip tank containing cooled thermal water.

### *Hot Springs*

Hot springs (37-83°C) in the Sevier Thermal Belt and groundwater wells in the North Milford valley were sampled for water. All sites were easy to access by vehicle. Hot spring waters were collected in beakers dipped in pools close to discharge points and then treated before filling HDP

This report is written for public disclosure.

bottles. Groundwater well samples were collected at the well head where aquifer fluids are pumped to the surface.

#### *Oil-gas production wells*

Oil and gas production wells were sampled for produced waters from the wellhead or separators (large tanks). Some separators have a valve located on the bottom of the tank, which permitted acquisition of a relatively pure water sample. Some separators and tanks were only accessible from the top, and to acquire a water sample, a bailer was lowered to the bottom of a tank through a layer of liquid hydrocarbon. Where the wellhead fluid could be sampled, a mixture of hydrocarbons and water were collected into a large clean bucket. Field treatment of samples was impractical, and most were contaminated with hydrocarbons. Hence, water samples were refined in the lab by letting them stand for 48 hours to allow immiscible liquid hydrocarbon to rise and separate from the underlying water, after which aliquots of water were decanted and treated. Three wells were directly sampled for helium and helium isotopes by filling copper tubes with water as described above.

#### *Water Samples*

For hot springs and geothermal production wells, two types of water samples were collected, treated and untreated.

Treated waters were filtered using a 0.45 um Millipore filter kit, and then acidified with nitric acid (HNO<sub>3</sub>) to pH 2 before filling HDP plastic bottles. All HDP bottles were acid cleaned (24 hours, 10% HCl) prior to filling with filtered water samples. To check for contamination, field blanks were prepared (Beowawe, Lightning Dock, Neal Hot Springs, Raft River, San Emidio) in which DDI water from the lab was carried into the field and then subjected to field filtration and acidification. Production fluids from the Uinta and Paradox Basins were collected in 1 gallon plastic bottles that had only contained Arrowhead spring water. Both the water and DDI water stored in a clean empty bottle were analyzed to check for potential contamination. No obvious sources of contamination from treatment and storage of samples were detected (Table 2; Tab-Field-Sample Blanks for QC).

Untreated waters were collected in glass bottles fitted with a rubber tube extension and a clamp. These waters were only analyzed for pH and bicarbonate. The bottle is filled with hot water to the top of the rubber tube extension (10-20 cm long) and then clamped. As the hot water cools and contracts, the rubber tube collapses, preventing the formation of an air gap; this ensures that the CO<sub>2</sub> concentration is preserved for the pH and bicarbonate analysis.

#### *Rock Samples*

Rock samples were collected from drill cuttings and field outcrops. Drill cuttings were available from the EGI core library for wells drilled at Beowawe, Dixie Valley, and Roosevelt Hot Springs. Mineralogic and lithologic characterizations of most of these samples are summarized (Table 4). Drill cuttings from wells drilled in the Uinta and Paradox Basins were obtained from the Utah Geological Survey, and these were selected to represent likely hydrocarbon reservoir and source rocks. Outcrop samples in the Sevier thermal belt were obtained from exposures of reservoir host rocks, volcanic rocks, and travertine deposits.

This report is written for public disclosure.

### *Pipe Scales*

Samples of pipe scales made of calcite were supplied by Terra-Gen from two wells (unknown depth) at Dixie Valley. These scales formed on small diameter coiled tubing that had been inserted into the well to continuously supply anti-scalant to the feed points at reservoir depths. The calcite likely deposited due to boiling and separation of gas from the liquid.

## **ANALYTICAL METHODS**

Four separate geochemical laboratories were used to acquire geochemical data, and the analytes and equipment utilized are summarized below.

### *Produced Water Samples*

Aliquots (50ml) of filtered and acidified water were submitted for analysis at the University of Minnesota geochemistry lab supervised by Professor Bill Seyfried. Major elements (Li, Na, K, Ca, Mg, SiO<sub>2</sub>) were analyzed using a Thermo Scientific iCAP 6000 series ICP-OES, and major anions (Cl, F, SO<sub>4</sub>) were analyzed using a Dionex ICS 5000+ ion chromatography system. Minor and trace cations were analyzed using a Thermo Scientific XSeries 2 ICP-MS. One suite (B, Ge, Sr, Nb, Mo, Ru, Rh, Pd, In, Sb, Te, Ta, W, Re, Ir, Pt and Au) was analyzed in standard mode in a matrix of trace metal grade 2% HNO<sub>3</sub>, 1% HCl, and 0.05% HF, whereas the second suite (Al, Sc, Mn, Fe, Co, Ni, Cu, Ga, As, Se, Rb, Y, Ag, Cd, Cs, La, Ce, Pr, Nd, Sm, Eu, Gd, Tb, Dy, Ho, Er, Tm, Yb, Lu, Tl, Pb, Th, U) was analyzed in CCT/KED mode in a matrix of trace metal grade 2% HNO<sub>3</sub>. Blanks and standards for trace elements covering a range of concentrations, from 0.01 to 100 ug/kg, were prepared and utilized for calibrating analytical results. The detection limits for trace elements, transition metals, and metalloids are 100 ug/kg (Li), 1-2 ug/kg (Al & Se), 0.1-0.2 ug/kg (Sr, Mn, Fe, Ge, As, W, Au), 0.05 ug/kg (Sc, Co, Ni, Cu, Ga, Y, Nb, Mo, Ru, Rh, Pd, Ag, Cd, Sb, Te, Ta, Rh, Ir, Pt, Tl, Pb), 0.01 ug/kg (In, La, Ce, Pr, Nd, Sm, Eu, Gd, Tb, Dy, Ho, Er, Tm, Yb, Lu, Th, U). At these detection limits, the accuracy and precision of results for standards is within 20% of their known elemental concentrations. Untreated waters were analyzed for pH and bicarbonate at the Utah Public Health laboratory in Salt Lake City.

### *Gas Samples*

Gas samples were analyzed at the University of New Mexico in the gas geochemistry lab supervised by Professor Tobias Fischer. Non-condensable gases (N<sub>2</sub>, H<sub>2</sub>, Ar, He, O<sub>2</sub>, CH<sub>4</sub>) were analyzed by gas chromatography, and CO<sub>2</sub> and H<sub>2</sub>S were analyzed by wet chemical titrations. The O<sub>2</sub> result was used to correct all the analyses for air contamination, which proved to be minor.

### *Helium and Helium Isotopes*

Copper tube water samples were analyzed for helium and helium isotopes by mass spectroscopy in the noble gas laboratory supervised by Professor Kip Solomon, Department of Geology and Geophysics, University of Utah.

This report is written for public disclosure.

### *Rock Samples, Drill Cuttings and Pipe Scales*

Rock samples (~1.5 grams of rock) were submitted for analysis at the University of Minnesota geochemistry lab supervised by Professor Bill Seyfried. They were dissolved into an aqueous solution using strong acids (HCl, HNO<sub>3</sub>, HF), sealed vessels, and a CEM SP-D Discover microwave digester. The solutions were analyzed for trace elements (Sc, Co, Cu, Zn, Ga, Ge, As, Se, Y, Nb, Ru, Rh, Pd, In, Sb, Te, La, Ce, Pr, Nd, Sm, Eu, Gd, Tb, Dy, Ho, Er, Tm, Yb, Lu, Re, Ir, Pt, Au, Pb) via standard addition in CCT/KED mode using a Thermo Scientific XSeries 2 ICP-MS. Hawaiian island basalt BHVO-1 and organic rich Cody shale (Sco-1) were used as standards to calibrate accuracy and precision. Many elements, including Sc, Co, Cu, Zn, Nb, Sb, La, Sm, Eu, Gd, Tb, Dy, Ho, Er, Tm and Yb, were within 20% accuracy and precision. The analytical results for some elements, namely As, Ru, Rh, Sb, Te, showed much stronger variance in precision exceeding 50%. Data for some elements, including Ge, Ru, Rh, Pd, In, Te, Re, Ir, Pt, and Au, are missing from the reported compositions of the standards, so concentrations for these elements are best viewed semi-quantitatively, with order of magnitude accuracy.

## **SCVM CONCENTRATIONS AND INVENTORIES IN PRODUCED FLUIDS**

The analytical results are presented in two parts. The first provides an overview of the general chemical characteristics of the produced water compositions. The second summarizes the concentrations, grades and inventories of SCVMs in produced waters.

### *General Chemical Characteristics of Produced Water Compositions*

All of the produced geothermal waters are near neutral pH, and they plot close to the meteoric water line, based on oxygen and hydrogen stable isotope ratios (Fig. 8). The slight positive  $\delta^{18}\text{O}$  enrichment reflects a commonly observed effect resulting from water-rock isotope exchange at elevated temperature (Craig, 1963). The strongest  $\delta^{18}\text{O}$  enrichments are found at Beowawe, Dixie Valley, Patua, Roosevelt Hot Springs, San Emidio, and Soda Lake, and these correlate with the hottest reservoir temperatures. Overall, the produced geothermal waters all appear to have a localized origin, reflecting deep circulation of local meteoric waters. The produced waters from the Uinta and Paradox Basins are also enriched in  $\delta^{18}\text{O}$ , and the positively sloping arrays of data (Fig. 8) are a typical feature of basinal waters, suggesting a relatively long period of storage in subsurface reservoir rocks (e.g., Taylor, 1997).

Using a classification scheme based on the concentrations of major anions, the waters from Blue Mountain, Dixie Valley, Patua, Raft River, Roosevelt Hot Springs, San Emidio, and Soda Lake are chloride waters (Fig. 9), which is typical of many high temperature geothermal waters (e.g., Giggenbach, 1997). The other geothermal waters (Beowawe, Lightning Dock, Neals Hot Spring, Newcastle, Thermo, and Tularosa) plot in the sulfate and bicarbonate fields, and this likely reflects the influence of soluble carbonate and sulfate-bearing minerals associated with sedimentary rocks. The waters from the Paradox Basin have the highest concentrations of total dissolved salts in the range of 65,000-130,000 ppm, dominated by chloride, whereas the Uinta basin waters have total dissolved salts in the range of 1000 to 40,000 ppm, which in most (not all) samples are dominated by chloride as well.

This report is written for public disclosure.

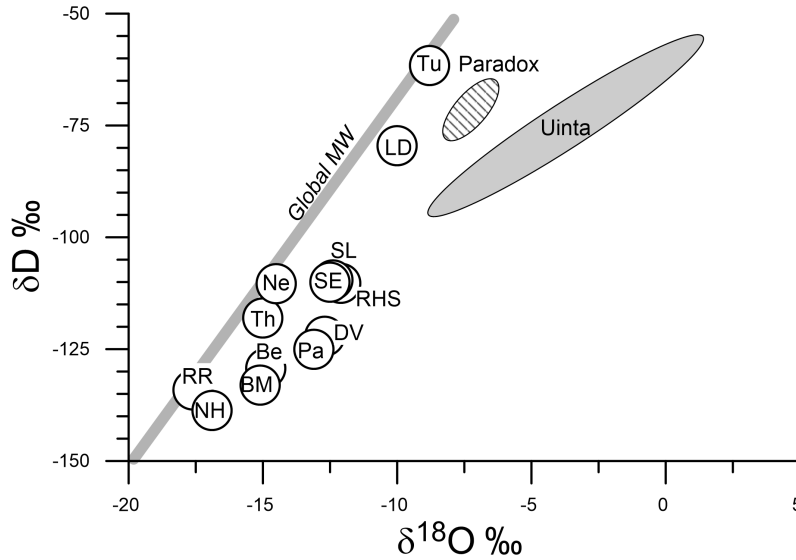


Figure 8. Stable isotope compositions of produced waters from geothermal and oil/gas wells. Abbreviations: Be=Beowawe; BM=Blue Mountain; DV=Dixie Valley; LD=Lightning Dock; Ne=Newcastle; NH=Neal Hot Springs; Pa=Patua; RHS=Roosvelt Hot Springs; RR=Raft River; SE=San Emidio; SL=Soda Lake; Th=Thermo; Tu=Tularosa.

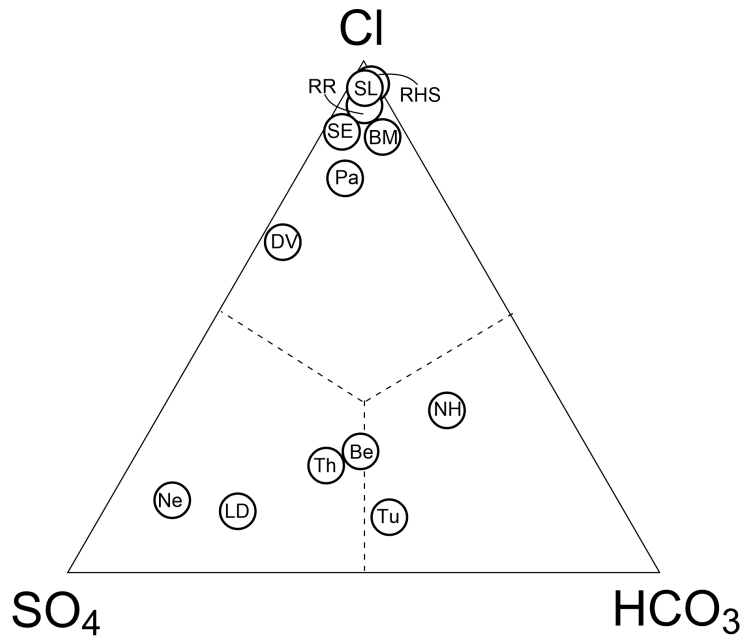


Figure 9. Relative concentrations of major dissolved anions in produced geothermal waters. Abbreviations: Be=Beowawe; BM=Blue Mountain; DV=Dixie Valley; LD=Lightning Dock; Ne=Newcastle; NH=Neal Hot Springs; Pa=Patua; RHS=Roosvelt Hot Springs; RR=Raft River; SE=San Emidio; SL=Soda Lake; Th=Thermo; Tu=Tularosa.

This report is written for public disclosure.

### *SCVM Concentrations & Inventories in Produced Waters*

As compiled in Table 2, the concentrations of most SCVM in produced waters range from <0.1 to 100 ug/kg (parts per billion-ppb). The main exception is lithium, which has concentrations that range from 100 to 26,000 ug/kg. Other elements that attain relatively high concentrations are gallium (10-80 ug/kg geothermal; 10-10,000 ug/kg Uinta and Paradox Basins), germanium (1-70 ug/kg geothermal; 10-500 ug/kg Uinta and Paradox Basins), scandium (0.1-2.0 ug/kg geothermal; 5-10 ug/kg Uinta and Paradox Basins), selenium (1-100 ug/kg geothermal; 10-20,000 ug/kg Uinta and Paradox Basins), and tellurium (0.1-10 ug/kg geothermal; 0.1-500 ug/kg Uinta and Paradox Basins). Small concentrations of rhodium in the range of 0.1-1.0 ug/kg were measured in water samples from Roosevelt Hot Springs, San Emidio, Soda Lake, and the Sevier thermal belt, and up to 10 ug/kg in Uinta and Paradox basin waters. Iridium concentrations of 0.1-0.3 ug/kg were measured in water samples from Patua and the Uinta Basin. Geothermal waters contain very low concentrations of REEs, below the analytical detection limits of 0.01 ug/kg, in accord with large amounts of published data on neutral pH thermal waters (Neupane and Wendt, 2017). The concentrations of some REEs in Uinta Basin waters, by contrast, range from 0.05 to 5 ppb, notably lanthanum, cerium, and europium. The concentrations of REEs in the Paradox Basin waters were below detection, which because of the high TDS was probably on the order of 0.15 ug/kg.

Inventories of SCVM in geothermal reservoir waters were calculated by multiplying the average concentrations in produced fluids by the reservoir volume, assuming a porosity of 15% (Table 2). The reservoir volume was estimated from the plan distribution of production wells multiplied by 1 km, which represents an arbitrarily assigned, but not geologically unreasonable, reservoir thickness. In the case of the Uinta and Paradox Basin wells, the known histories of water production were used to calculate the reservoir water volumes. Figures 10, 11 and 12 graphically portray the concentrations of gallium, germanium, lithium, scandium, selenium, and tellurium versus reservoir inventories. Among the geothermal fields, the Roosevelt Hot Spring reservoir appears to have the largest endowments of germanium (20,000 kg) and lithium (7 million kg), the Patua reservoir appears to have the largest endowments of gallium (25,000 kg), selenium (47,000 kg), and tellurium (2500 kg), and the Raft River reservoir appears to have the large endowment of scandium (700 kg). By comparison, the Uinta Basin has larger inventories of gallium (>100,000 kg).

All reported values of SCVM concentrations and inventories are provisional. The reliability of the geochemical data needs to be checked with multiple repeat analyses to test for uniformity and consistency of elemental concentrations, and the reservoir volumes need to be confirmed based on information held by field operators regarding the occurrence and distributions of production well feed zones. Furthermore, some production waters are modified by injection of additives, and these need to be checked as possible sources of SCVM elements.

This report is written for public disclosure.

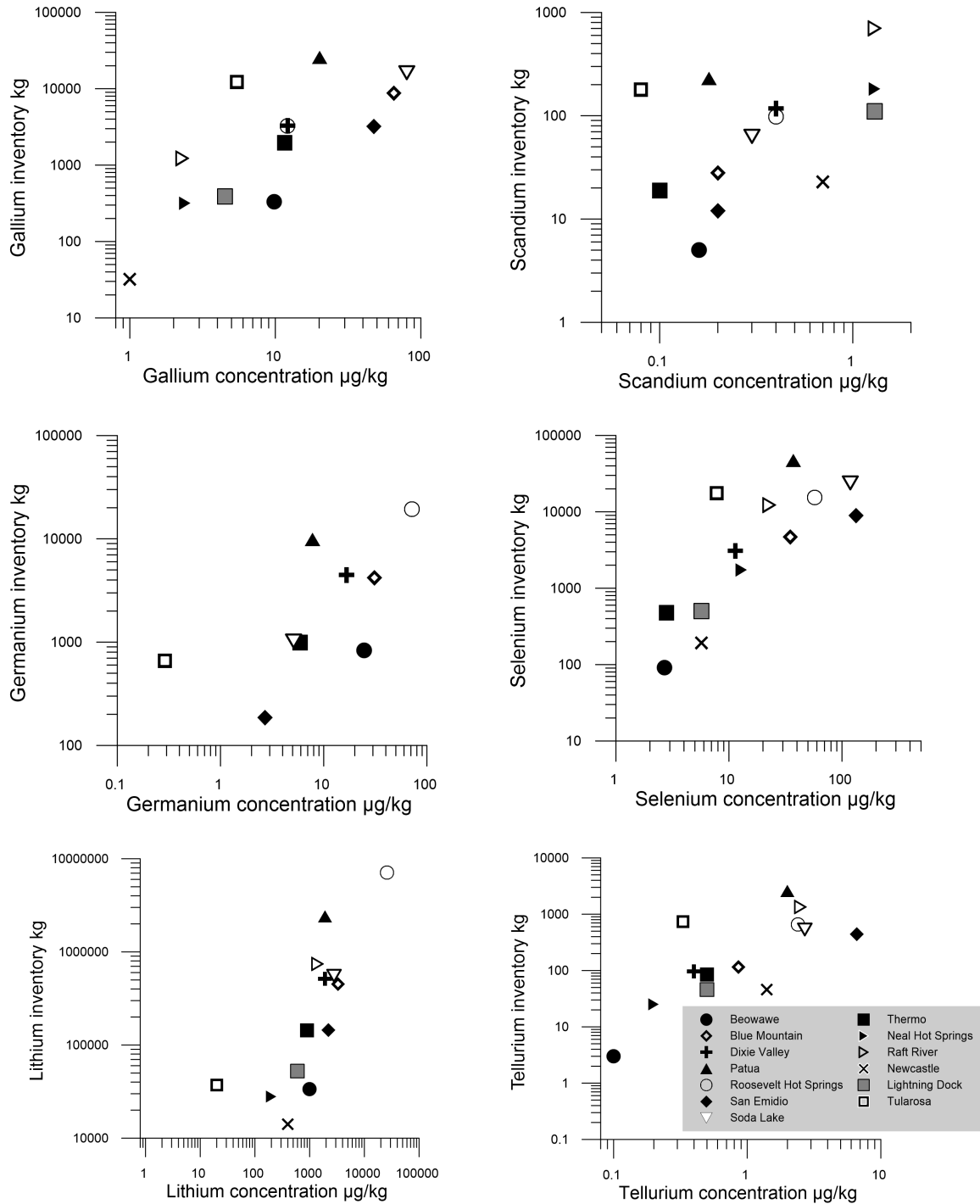


Figure 10. Average concentrations ( $\mu\text{g/kg}$  or ppb) of gallium, germanium, lithium, scandium, selenium, and tellurium in produced waters from geothermal fields plotted against estimated reservoir inventories.

This report is written for public disclosure.

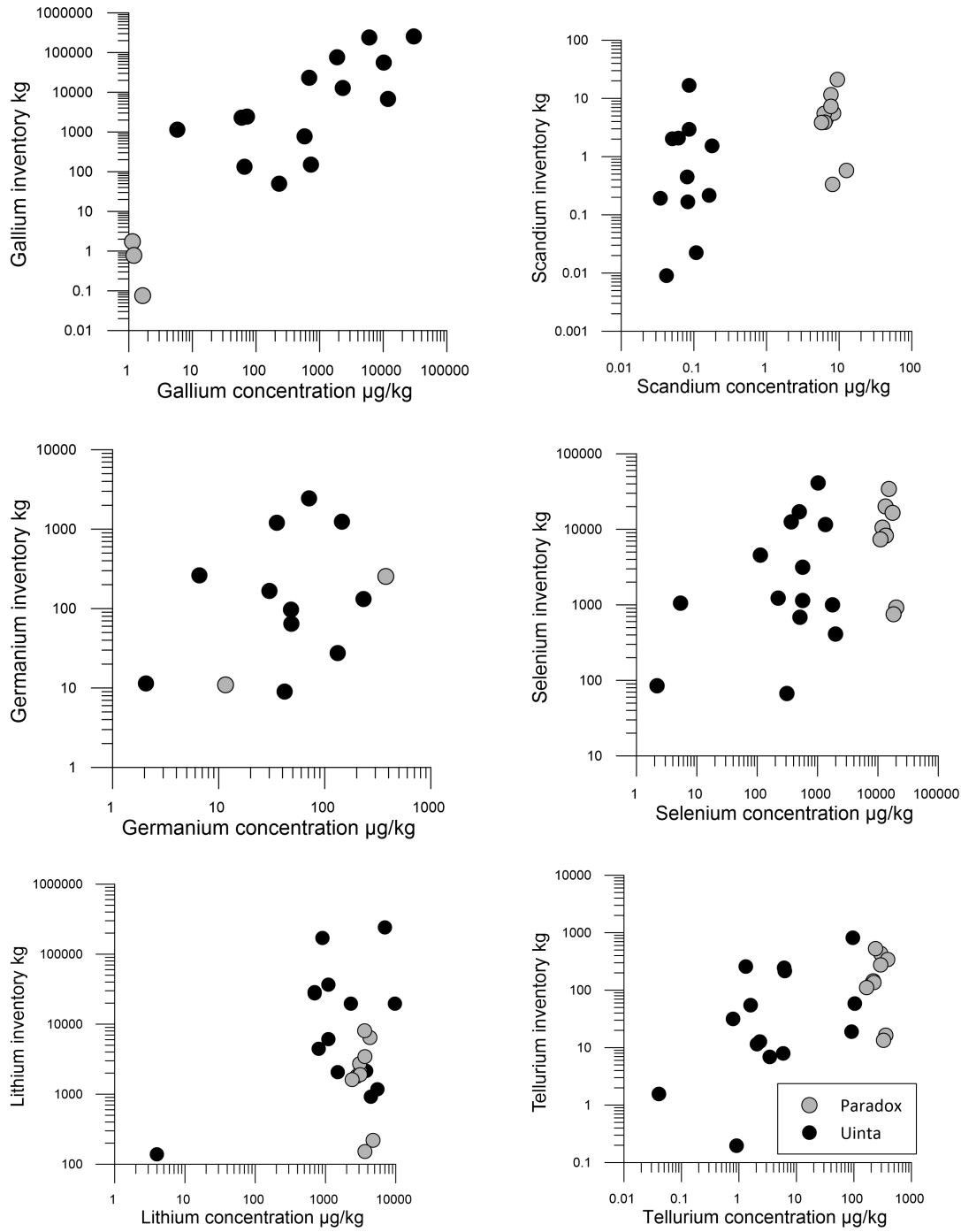


Figure 11. Concentrations ( $\mu\text{g/kg}$  or ppb) of gallium, germanium, lithium, scandium, selenium, and tellurium in produced waters from the Uinta and Paradox Basins plotted against estimated reservoir inventories.

This report is written for public disclosure.

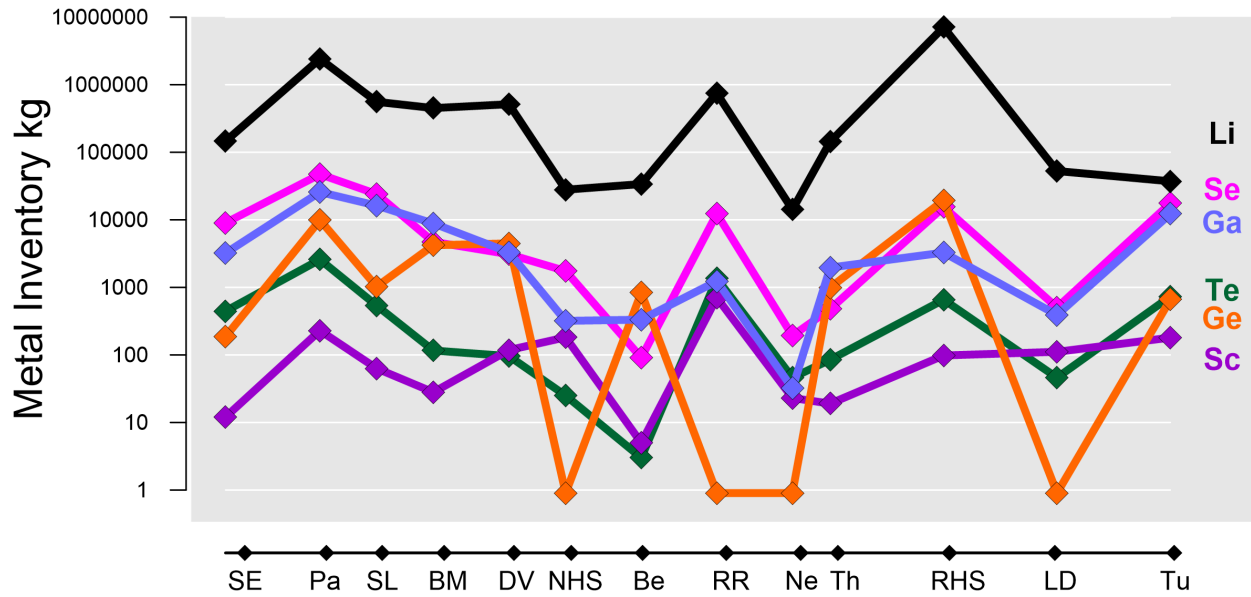


Figure 12. Calculated inventories (kg) of gallium, germanium, lithium, scandium, selenium, and tellurium in produced waters from geothermal reservoirs. Abbreviations: B=Beowawe; BM=Blue Mountain; DV=Dixie Valley; P=Patua; RHS=Roosvelt Hot Springs; SE=San Emidio; SL=Soda Lake; T=Thermo.

This report is written for public disclosure.

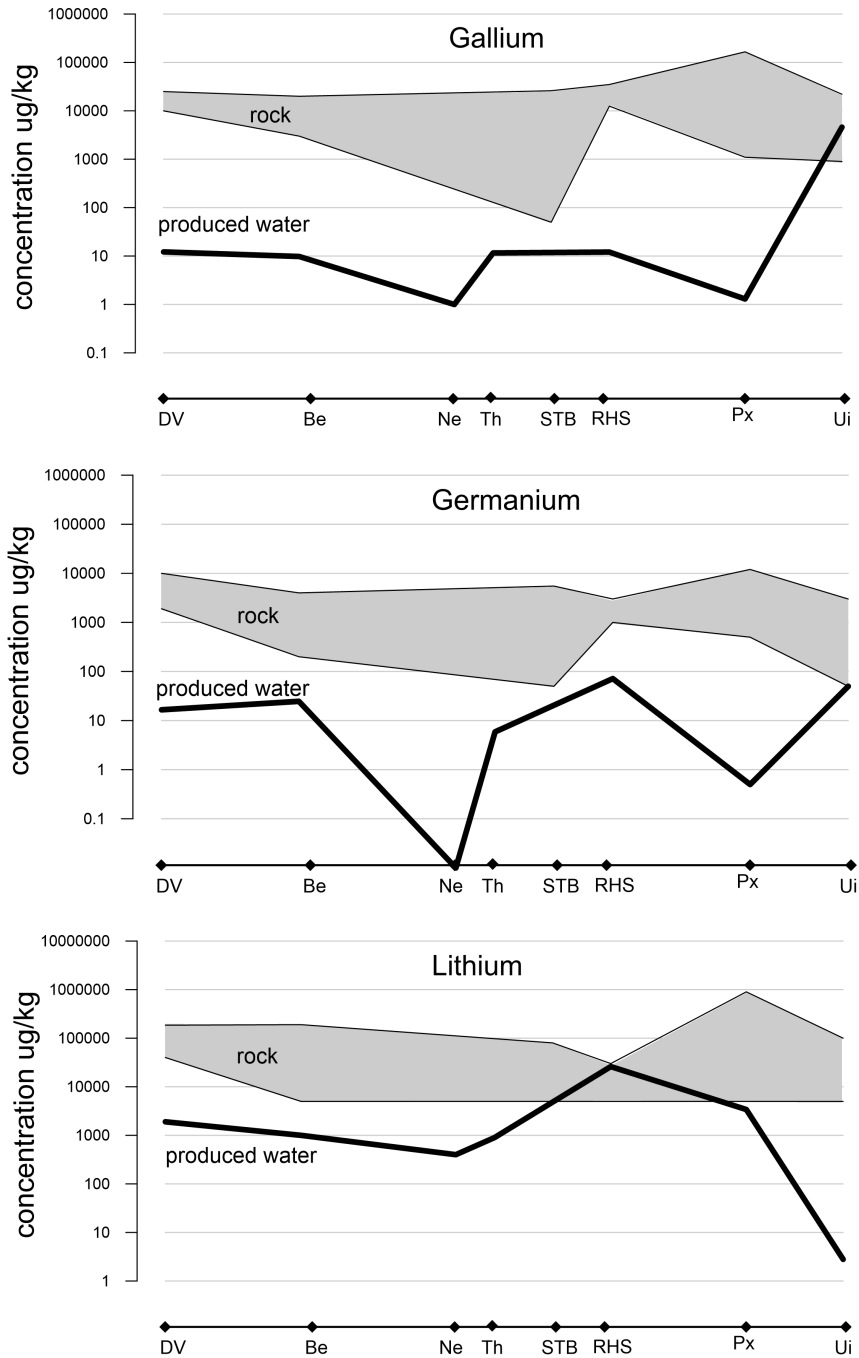


Figure 13a. Comparison of the range of concentrations of gallium, germanium and lithium in produced geothermal waters and in rock samples collected from wells at Dixie Valley (DV), Beowawe (Be), Roosevelt Hot Springs (RHS), Paradox Basin (Px) and Uinta Basin (UI).

This report is written for public disclosure.

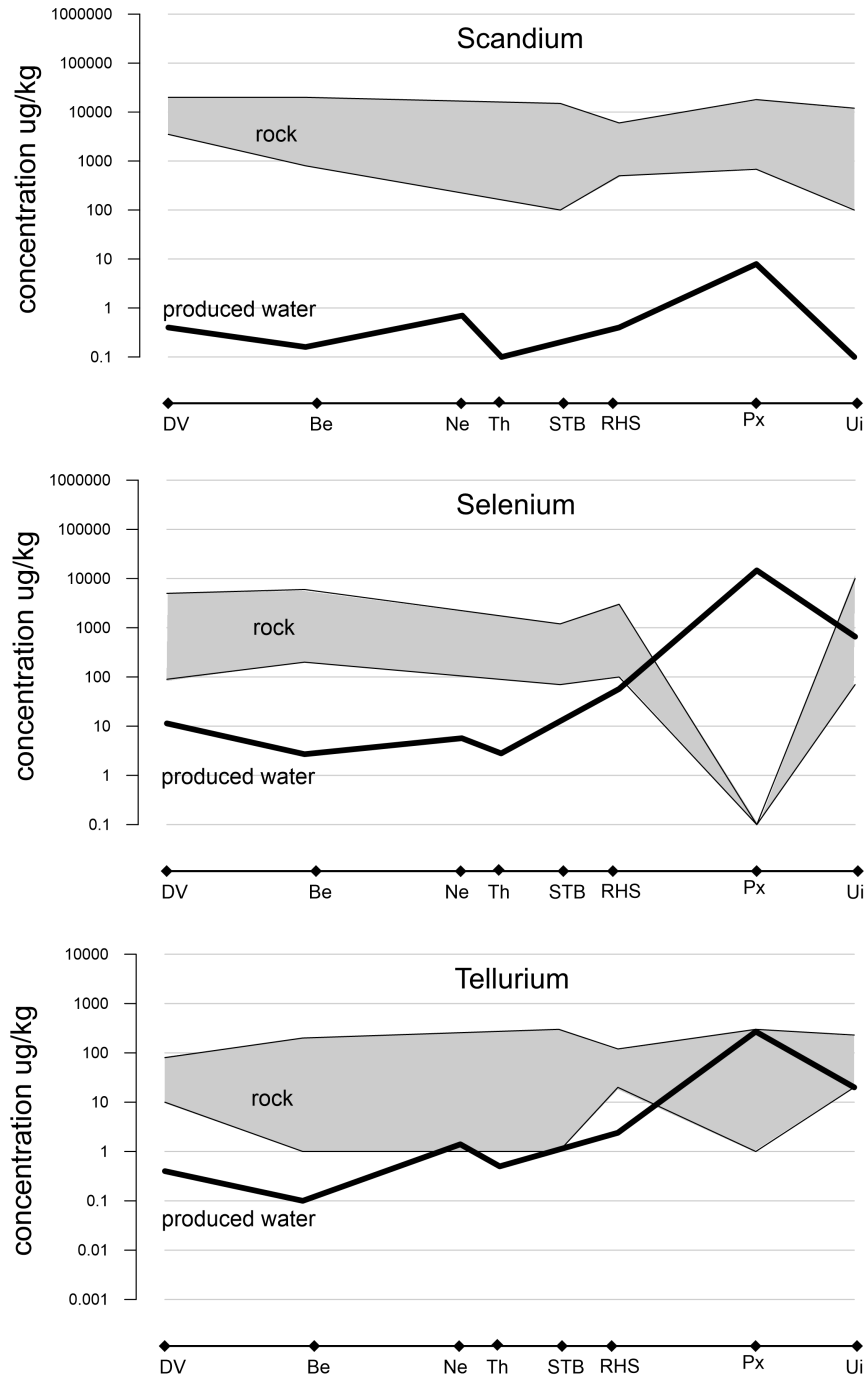


Figure 13b. Comparison of the range of concentrations of scandium, selenium, and tellurium in produced geothermal waters and in rock samples collected from wells at Dixie Valley (DV), Beowawe (Be), Roosevelt Hot Springs (RHS), Paradox Basin (Px) and Uinta Basin (UI).

This report is written for public disclosure.

The ranges of gallium, germanium, lithium, scandium, selenium, and tellurium concentrations in rock samples are graphically portrayed along with concentrations of these elements in produced waters in Figure 13. The aqueous elemental concentrations are generally much lower than the rock concentrations. Furthermore, the aqueous and rock concentrations show poor correlation, especially selenium and tellurium in the Paradox Basin samples. These data trends suggest that there is no direct relationship between the concentrations of SCVMs in rocks versus produced waters.

To test the possibility that some SCVM elements might be depositing as scales in geothermal wells (e.g., Simmons et al., 2016b), six samples of calcite scale from Dixie Valley were analyzed. One sample (28-33A; Table 3-Tab Dixie Valley Calcite Scales) contains anomalous concentrations of cobalt (4,000 ug/kg), gallium (800 ug/kg), germanium (45 ug/kg), selenium (14,000 ug/kg), tellurium (4000 ug/kg), gold (20,000 ug/kg) and palladium (500 ug/kg). Trace amounts (10-100 ug/kg) of yttrium, niobium, rhodium, lanthanum, cerium, neodymium, europium, gadolinium, and rhenium were also measured. These data suggest that some SCVM deposit from produced fluids before reaching the surface, likely due to boiling in the well. A comparison of the data for produced waters, calcite scales, and subsurface rocks based on drill cuttings is shown in Figure 14. Calcite precipitation in the well appears to be very effective at concentrating most elements from produced geothermal water, except for As and Sb. Thus, where flashing or boiling is occurring in self-flowing wells (i.e. Beowawe, Dixie Valley, and Roosevelt Hot Springs), a significant portion of the reservoir aqueous SCVM might be sequestered in scales before reaching the surface.

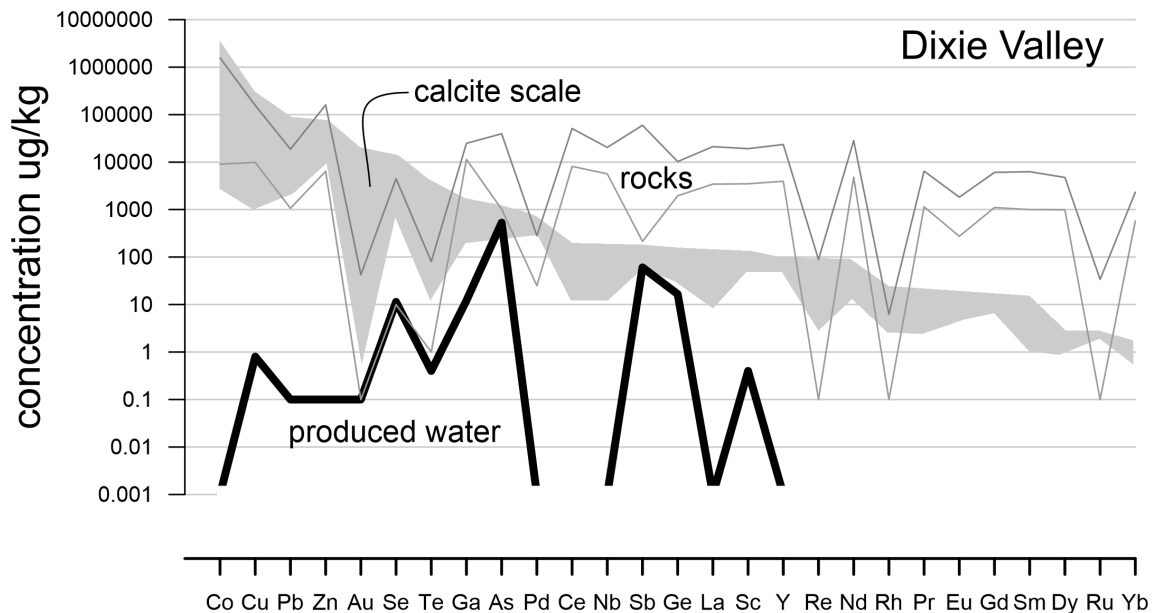


Figure 14. Comparison of the range of concentrations of metals in produced geothermal waters (black bold line), calcite scales (grey-filled area) and subsurface lithologies based on drill cuttings (rocks-white filled area between thin black lines) from wells at Dixie Valley.

This report is written for public disclosure.

Helium isotope analyses were obtained for produced waters samples collected at several fields (Fig. 15). Along with isotope ratios, reported as R/Ra values (where  $R=^3\text{He}/^4\text{He}$  sample and  $Ra=^3\text{He}/^4\text{He}$  atmosphere), helium inventories were also calculated based on concentrations of helium in the water samples. The results show that helium inventory values range widely, with the highest occurring at Patua and Raft River. By contrast, the highest R/Ra values are found at Soda Lake (R/Ra=4.5) and Roosevelt Hot Springs (R/Ra=2.1).

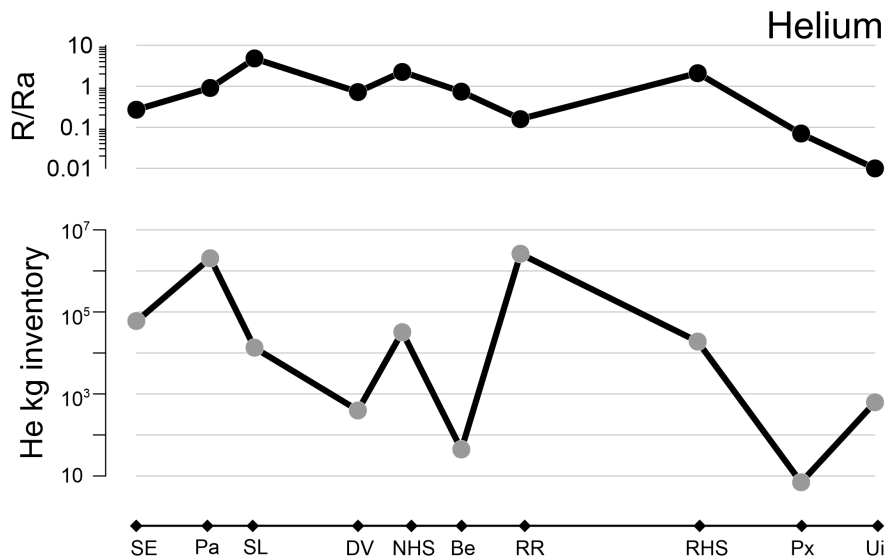


Figure 15. Calculated inventories of helium and helium isotope ratios (R/Ra) determined from produced water samples collected from wells at San Emidio (SE), Patua (Pa), Soda Lake (SL), Dixie Valley (DV), Neal Hot Spring (NHS), Beowawe (Be), Raft River (RR), Roosevelt Hot Springs (RHS), Paradox Basin (Px) and Uinta Basin (UI).

### PROCESSES CONTROLLING SCVM IN THE SEVIER THERMAL BELT: PRELIMINARY ASSESSMENT

The Sevier Thermal Belt, southwestern Utah, covers 20,000 km<sup>2</sup> and is located along the eastern edge of the Great Basin; it encompasses geothermal production fields at Cove Fort, Roosevelt Hot Springs, and Thermo, plus scattered hot spring activity, and the Covenant oil field (Fig. 16). Regionally, the belt is characterized by elevated heat flow, active seismicity, and Quaternary basalt-rhyolite magmatism (Mabey and Budding, 1987; Blackett and Wakefield, 2002). This province has been the subject of several investigations, including geothermal play fairway analysis, geothermal resources in hot sedimentary aquifers, and development of a FORGE laboratory site (e.g. Allis et al., 2015; Simmons et al., 2015, 2016a, 2019; Wannamaker et al., 2016). By comparing results from this relatively compact region, the potential first order controls on SCVM behavior in produced thermal waters are evaluated.

This report is written for public disclosure.

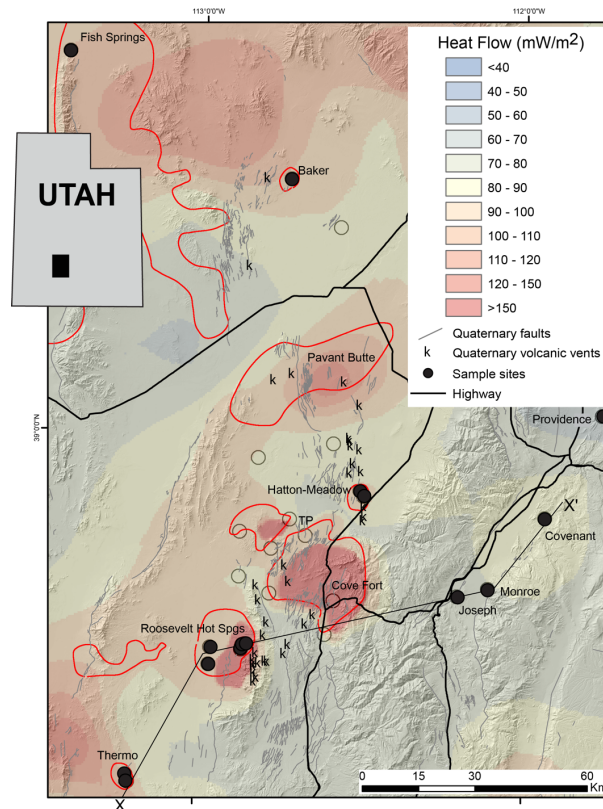


Figure 16. Physiographic and heat flow map of the Sevier Thermal Belt, showing the locations of geothermal fields, hot springs (labeled black filled circles), Quaternary faults, and Quaternary volcanic centers; TP stand for Twin Peaks referred to in the text. Heat flow patterns are based on a regional analysis by Gwynn et al. (2018) and Allis et al. (2017; 2018). The heat flow results are based on bottom hole temperatures of numerous wells, measured vertical temperature gradients, and thermal characteristics of rocks in wells. The continuous red line marks the limit where subsurface temperature is  $\geq 20^\circ\text{C}$  at 100 m (Gwynn et al., 2018).

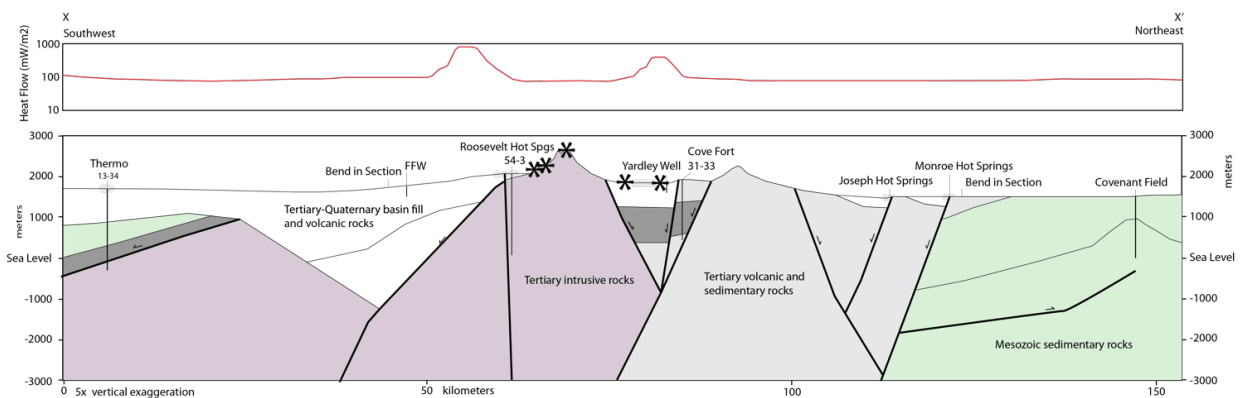


Figure 17. Geologic cross section showing the setting of the three producing geothermal fields in the southern part of the study area and the corresponding heat flow (Kirby, 2012; Gwynn et al., 2018). The asterisks mark Quaternary volcanic centers.

This report is written for public disclosure.

### *Geologic Setting*

The geology of the area is summarized in Hintze et al. (2000) and Hintze and Davis (2003). The area covers a zone of tectonic transition that grades west to east from the thinned, normally faulted crust of the Basin and Range province to the largely intact and stable crust of the Colorado Plateau (Wannamaker et al., 2001, 2008). The main rock types include Precambrian clastic rocks, Paleozoic carbonates, Mesozoic and Cenozoic clastic sedimentary rocks, and Cenozoic volcanic rocks, that make up the mountain ranges of the Sevier Desert. The intervening wide low relief valleys are floored by Tertiary-Quaternary lacustrine and alluvial basin-fill and volcanic units. Significant magmatism began during the Oligocene with the growth and emplacement of a series of large volcanic centers in the southeast part of the area. The rate and volume of magmatism has decreased through time but continues today as a series of Quaternary volcanic centers. The structural evolution of the area is complicated and polyphase, involving protracted periods of shortening and extension. The bedrock was deformed by late Jurassic through Eocene tectonic compression, which produced the Sevier fold and thrust belt. Basin and Range extension began during the Miocene and continues to the present. Owing to the long-lived tectonism, structures include shallowly dipping thrust faults and normal faults and steeply dipping normal faults, with attendant bedrock fracturing. Many of the hot spring areas as well as the three major geothermal resources, Roosevelt Hot Springs, Cove Fort, and Thermo, are associated with fault-related hydrothermal activity shown in Figure 17.

### *Chemical and Isotopic Compositions of Thermal Waters*

Analytical results of a regional sampling campaign commencing 2015 are graphically portrayed in Figures 18 through 22. These data are based on samples of water collected from cold springs and groundwater wells, hot springs, geothermal production wells, and oil and gas wells.

The stable isotope data in Figure 18 show that cold groundwater generally follows or lies slightly to the right of the global meteoric water line, and the wide range in compositions can be attributed to the effects of elevation and latitude over the study area (Craig, 1961). The hot spring waters and the geothermal production waters at Cove Fort and Thermo overlap these cold groundwater values, with small but variable  $\delta^{18}\text{O}$  enrichments likely caused by hydrothermal water-rock interaction (Craig, 1963). Monroe is the only hot spring water that plots almost directly on the meteoric water line, suggesting minimal high temperature interaction with country rocks. The Roosevelt Hot Springs production waters show the strongest  $\delta^{18}\text{O}$  enrichment, with a wide spread in values that reflects modification in the original reservoir water composition resulting from the effects of production related to steam-loss and injectate inmixing over the last 25 years (Simmons et al., 2018). Geothermal production waters from Cove Fort, Roosevelt Hot Springs, and Thermo clearly originate from local meteoric water recharge, but given that the modern local groundwaters have slightly heavier values, the produced water isotopic compositions likely reflect Pleistocene compositions (e.g., Flynn and Buchanan, 1993). Given the large geographic distance that separates them, the strong similarity in Cove Fort and Thermo water compositions is simply a coincidence. The Covenant water, which comes from a nearly pure quartz sandstone reservoir at  $\sim 90^\circ\text{C}$  (Parry et al., 2009), resembles the hot spring water compositions of Monroe and Joseph. By contrast, the Providence water composition

This report is written for public disclosure.

represents an anomalous outlier that may reflect extreme hydrogen enrichment due to isotope exchange with methane (e.g., Taylor, 1997).

The relative concentrations of chloride, bicarbonate, and sulfate indicate differences in the compositions of thermal waters compared to cold groundwaters (Fig. 19). Most of thermal waters can be classified as chloride, sulfate or hybrid chloride-sulfate waters, with TDS values that range between 1000 and 10,000 mg/kg. The cold groundwaters by contrast are generally more dilute, with 300 to 4500 mg/kg TDS, and contain proportionally much less sulfate and much more bicarbonate.

The noble gas isotopic ratios (Fig. 20) indicate that helium in most cold ground waters derives from air, the main exceptions being two samples near Twin Peaks and groundwater samples from the North Milford valley, which are discussed later. The Twin Peaks samples appear to be acquiring helium from a combination of air, crust and mantle sources. By contrast, the isotope ratios of most thermal waters form a distinct coherent array that represents a mixture of mantle and crustal sourced helium. Within this array, the highest R/Ra values of 2.1 to 2.2 measured at Roosevelt Hot Springs confirms the existence of a melt body of mantle origin beneath the hydrothermal system as inferred by previous workers (Kennedy and van Soest, 2006). The second highest R/Ra values of ~0.8 are measured on produced waters from Thermo and Cove Fort, and because of their relatively high  $^4\text{He}/^{20}\text{Ne}$  values, mantle origin melts might underlie these hydrothermal systems (e.g., Siler and Kennedy, 2016). The isotope ratio of Thermo hot spring reflects strong inmixing or contamination from air. The isotopic data for Baker, Monroe, and Joseph conform to the thermal water array, but have the low R/Ra values representing the weakest inputs of mantle He. Fish Springs is distinct, indicating a very strong input of crustal He. Lastly, the Providence sample appears to have incorporated a large amount of air, in which the water originally represented a mixture of crustal and mantle He.

The aqueous silica values are plotted against sampling and reservoir temperatures (Fig. 21), and the highest concentrations are associated with the hottest temperatures, reflecting strong influence of fluid-mineral equilibria with quartz or chalcedony, and showing the applicability of silica-mineral geothermometry (Fournier, 1991). The hot spring waters, however, have relatively low concentrations of silica, indicating relatively cool subsurface equilibration temperatures between 40 and 130° C, and this is consistent with the absence of apron deposits made of silica sinter. The cold ground waters have the lowest silica concentrations and the lowest equilibration temperatures.

The Na/K and K/Mg values like the aqueous silica concentrations are used here to interpret aqueous geothermometers and fluid-mineral equilibria (Figure 22). In this case, they are converted to Na/K and  $\text{K}^2/\text{Mg}$  equilibration temperatures rather than representing the Na-K-Mg values on a trilinear plot (Giggenbach, 1988). The Roosevelt Hot Springs waters plot the closest to the full equilibrium line, which reflects fluid-mineral equilibria involving quartz, K-feldspar, Na-feldspar, K-mica, and Mg-chlorite at ~300° C (Giggenbach, 1988) and which is consistent with hydrothermal alteration minerals occurring in the reservoir (Capuano and Cole, 1982). Thermal waters from Cove Fort and Thermo have  $\text{K}^2/\text{Mg}$  values that correlate with measured

This report is written for public disclosure.

reservoir temperatures, whereas the Na/K values suggest equilibration at deeper levels and  $>250^{\circ}\text{C}$ . Both thermal spring waters and cold groundwaters contain relatively high concentrations of Mg, and hence reflect cool  $\text{K}^2/\text{Mg}$  equilibration temperatures mostly in the range of  $20\text{-}100^{\circ}\text{C}$ . The Na/K values of hot spring waters range widely, and where they are low, the inferred hot equilibration temperatures seem unreliable; the cation ratios probably reflect partial dissolution of soluble salts in the basin sediments. The equilibration temperatures for Covenant and Providence waters exceed the measured reservoir temperatures, and hence they have minimal significance.

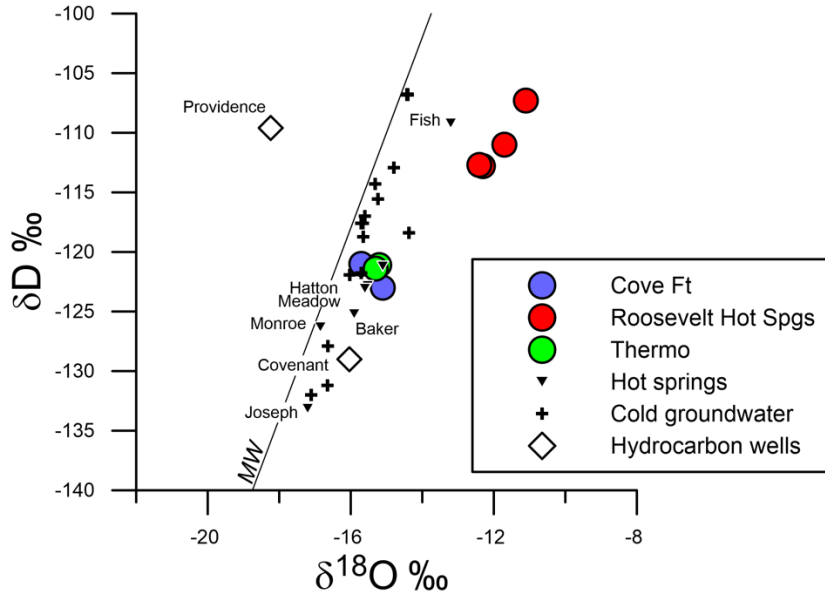


Figure 18: Stable isotope compositions of waters obtained from geothermal and oil-gas production wells, hot springs, cold springs and ground water wells.

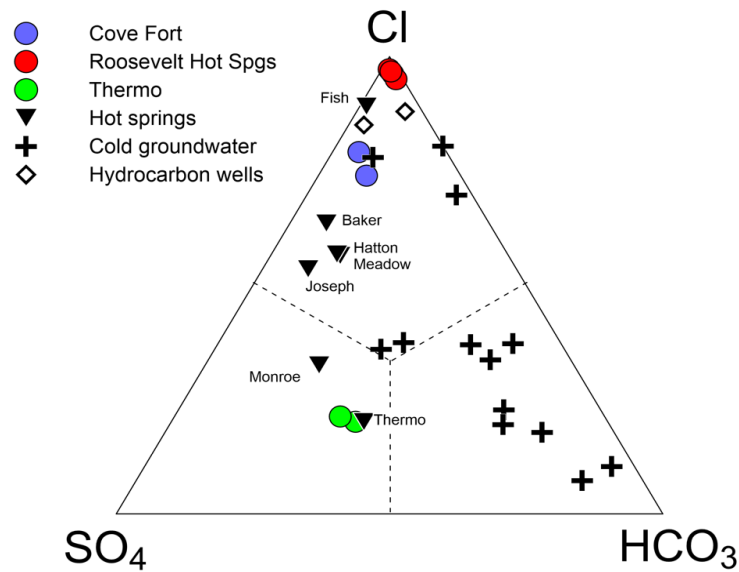


Figure 19: Relative concentrations of chloride, bicarbonate, and sulfate in water samples obtained from geothermal and oil-gas production wells, hot springs, cold springs and ground water wells.

This report is written for public disclosure.

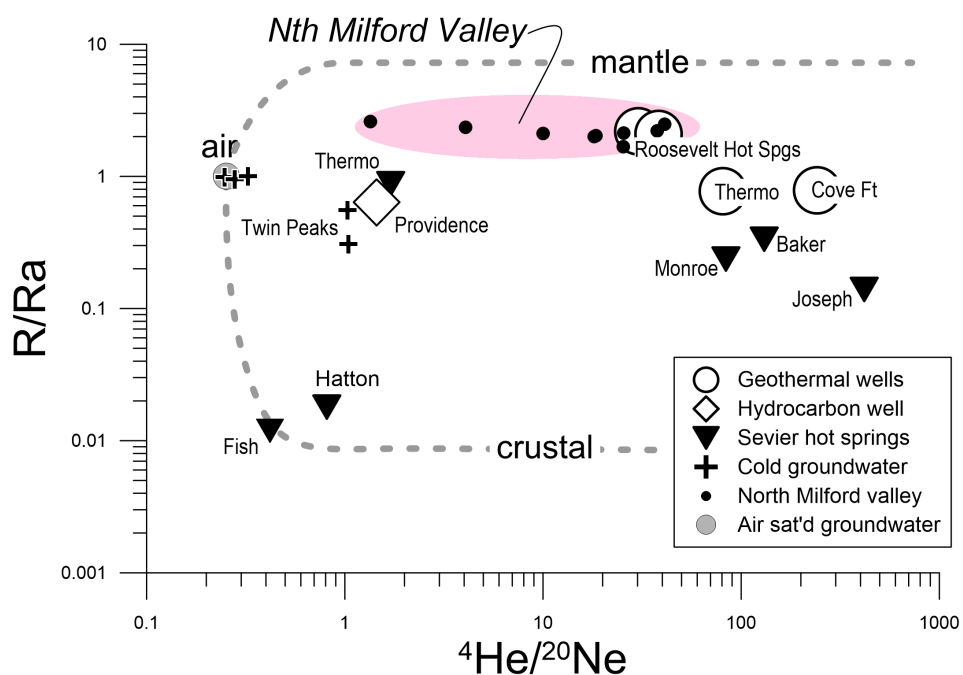


Figure 20: Helium and neon isotope compositions of waters obtained from geothermal and oil-gas production wells, hot springs, cold springs and ground water wells. Cove Fort data come from Tonani et al., 1998. The small black filled circles from the North Milford Valley represent helium isotope compositions in groundwater that have similar R/Ra values to Roosevelt Hot Springs.

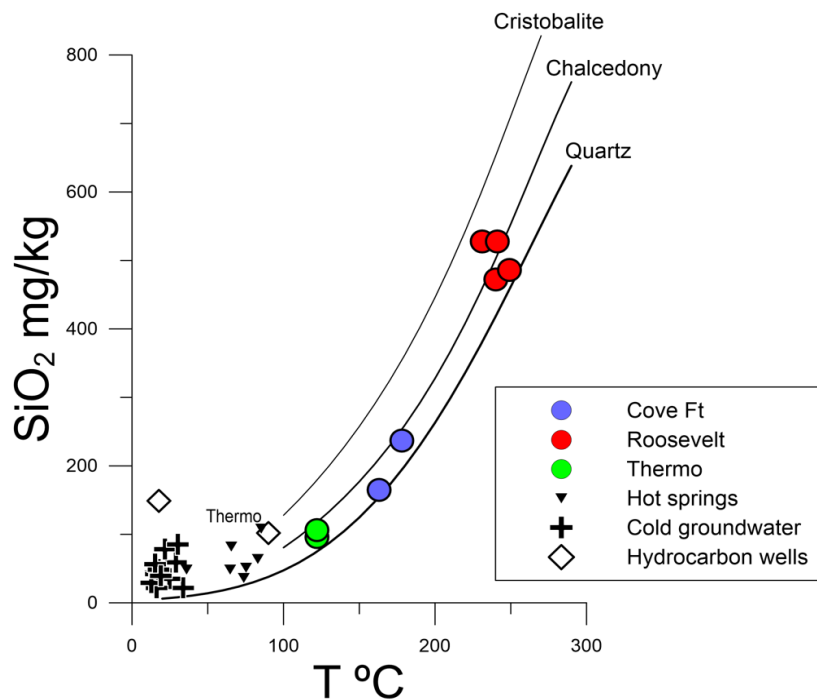


Figure 21: Aqueous silica concentration versus temperature for samples obtained from geothermal and oil-gas production wells, hot springs, cold springs and ground water wells.

This report is written for public disclosure.

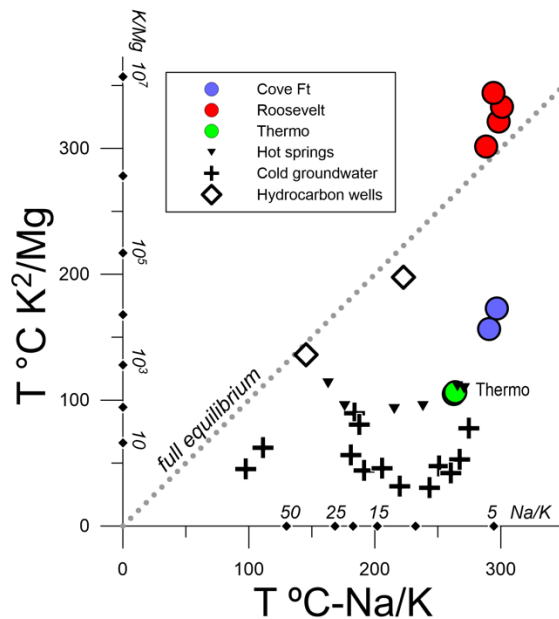


Figure 22: Na/K versus K/Mg values for samples obtained from geothermal and oil-gas production wells, hot springs, cold springs and ground water wells represented as geothermometer equilibration temperatures based on fluid-mineral equilibria (Giggenbach, 1988).

#### *Implications for Hydrothermal Fluid Flow*

The data above provide insights about deep to shallow level controls on hydrothermal activity in the Sevier Thermal Belt, which is relevant for understanding SCVM transport in hydrothermal solutions. There is a clear association between high enthalpy thermal fluids, mantle-sourced He, and deeply circulated meteoric water heated by intrusions of magma, as exemplified by Roosevelt Hot Springs, which is the hottest geothermal resource in the belt. From cation equilibration temperatures, the Roosevelt Hot Springs waters appear to be heated to  $>300^{\circ}\text{C}$ , which based on the conductive thermal gradient of  $70^{\circ}\text{C}/\text{km}$  at the nearby Utah FORGE site, suggests a minimum convection circulation depth of 4.5 km. Because the hydrothermal system is entirely hosted in granitic rock, the primary control on fluid flow from the base of the convection cell through the reservoir to the surface is a relatively narrow, subvertical fault-related fracture mesh. Thus, this one system represents a simple end-member condition for hydrothermal activity, involving deep magmatic intrusion and fluid upflow through a well-connected fracture network.

The hydrothermal activity and geothermal resources at Cove Fort and Thermo are also related to intrusions of magma, but with stronger inputs of radiogenic crustal sourced helium. At Cove Fort, the reservoir and quartz-silica equilibration temperatures are  $150\text{-}170^{\circ}\text{C}$ , but the overall thermal output is 110 MW, nearly twice that of Roosevelt Hot Springs (Allis et al., 2017). Although the Cove Fort geothermal resource appears to be cooler than Roosevelt Hot Springs, the total heat transfer to the surface is approximately two times greater. If the Na/K equilibration temperatures of  $\sim 300^{\circ}\text{C}$  are believable, then conceivably hotter conditions exist at deep levels in this system. The developed Cove Fort resource lies on the southeastern periphery of the regional heat flow anomaly, which means the hottest up-flowing part of Cove Fort has possibly not yet

This report is written for public disclosure.

been identified. From a geologic perspective, the fact that the reservoir is hosted in stratified sedimentary and volcanic rocks, means that fluid flow might be dispersed, with the effect of dissipating thermal energy across the shallow part of the system. Cove Fort also has a strong hydraulic gradient associated with the range front setting, and westward groundwater flow strongly influences the shape of the heat flow anomaly (Allis et al., 2017).

The Thermo geothermal reservoir is also hosted in stratified sedimentary rocks, with an even cooler resource and quartz-equilibration temperature of 120-130° C; the Na/K equilibration temperatures of ~300° C point to hotter conditions at depth, but there is no corresponding estimate of total thermal output. The reservoir is also underlain by granitic crystalline rock. Thus, deep fluid flow is likely controlled by an interconnected fracture network like Roosevelt Hot Springs. From the reservoir to the surface, rising fluids are modified by varying degrees of lateral dispersion through horizontally bedded strata combined with flow through shallow subvertical faults.

The noble gas data suggest hot spring waters at Joseph, Monroe, and Baker may be affiliated with magmatic heat sources too. The strongest supporting evidence exists at Baker, which lies on the east edge of the Crater basalt volcanic center and on the east edge of a large heat flow anomaly extending to Fish Springs. Although the aggregate thermal water flow at Baker indicates significant thermal output of ~20-45 MW, the quartz-equilibration temperature is <100° C, suggesting shallow (<3 km?) circulation of heated meteoric water. This might imply the existence of a stratigraphic barrier to fluid flow and heat transfer. Monroe and Joseph hot springs have no correlation with Quaternary volcanic activity, but they are associated with Quaternary faults within the transition zone of the Colorado Plateau. The hot spring discharges at Monroe (20 L/s, 5 MWth) and Joseph (2 L/s, 0.4 MWth) are modest and, although a deep magmatic heat source might exist, thermal outputs can be accounted for by shallow circulation through a sub-vertical fault.

By contrast to the above, helium data for Hatton (and Fish Springs) suggest heat transfer in these settings is amagmatic and entirely dependent on conductive heating of pore waters through relatively long-lived interaction with hot radiogenic crust. The Hatton-Meadow hot springs lack correlation with a regional heat flow anomaly, but possibly derive from a warm basin-fill aquifer at ~100° C.

In summary, the He isotope data indicate connections through to the upper mantle are developed over the region of strongest and most concentrated hydrothermal activity. By contrast, stable isotope data demonstrate that most of the convective heat transfer is associated with shallow to deep circulation of local meteoric water. Quartz-silica geothermometry suggests that convective heat transfer is compartmentalized by stratigraphic horizons and sub-vertical faults. In some cases, the regional hydraulic gradient generates outflow zones of hot water. Although the geology of the Sevier Thermal Belt is complex, geothermal activity is developed over a very large area in multiple sites, and fluid compositions are strongly influenced by localized effects of water-rock interactions and the availabilities of soluble metals and elements.

This report is written for public disclosure.

*Relationship between SCVM concentrations, Temperature, and TDS*

The two most basic controls on SCVM concentrations are likely to involve temperature and ionic strength (as reflected by total dissolved salts), given these generally control the solubilities of minerals and metals in hydrothermal fluids (e.g., Seward and Barnes, 1997). As a check for systematic variations, the values of total dissolved salts (TDS) for the Sevier Thermal Belt and all produced waters are plotted as a function of temperature (Fig. 23), and the results show a weak correlation. As becomes clear below, TDS and temperature seem to have only partial influence on the concentrations of SCVMs in hydrothermal solutions and produced waters.

In Figure 24, gallium, germanium, lithium, scandium, selenium and tellurium concentrations in produced geothermal waters are compared to Sevier Thermal Belt waters as a function of temperature. The first thing to note is that the Sevier Thermal Belt waters, in comparison to all the produced thermal waters, are generally low to intermediate in the range of concentrations of gallium, germanium, and scandium, similar to the range of concentrations for selenium and lithium, and higher in concentrations of tellurium. Secondly, the hottest production water at Roosevelt Hot Springs has the highest concentrations of germanium, lithium, and scandium, and close to the highest concentrations of selenium; by contrast, the relatively cool production water at Thermo is associated with low concentrations of gallium, germanium, lithium, scandium, selenium and tellurium. Thirdly, germanium and lithium show positive correlation with temperature, in contrast to gallium, scandium, selenium and tellurium, which show no correlation. From these trends, it seems that temperature control on the concentrations of SCVM elements is restricted to germanium and lithium.

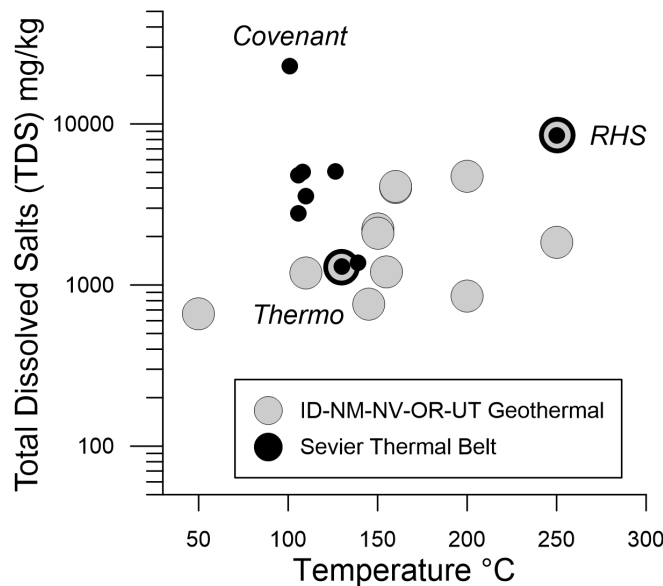


Figure 23. Total dissolved salt concentrations (mg/kg or ppm) of Sevier Thermal Belt and produced geothermal waters plotted against measured or quartz-silica equilibration temperatures (Table 2). The most saline water is from the Covenant oil field. Roosevelt Hot Springs (RHS) and Thermo samples are denoted by the black-filled circles, which are surrounded by larger grey-filled circles and bold black outlines.

This report is written for public disclosure.

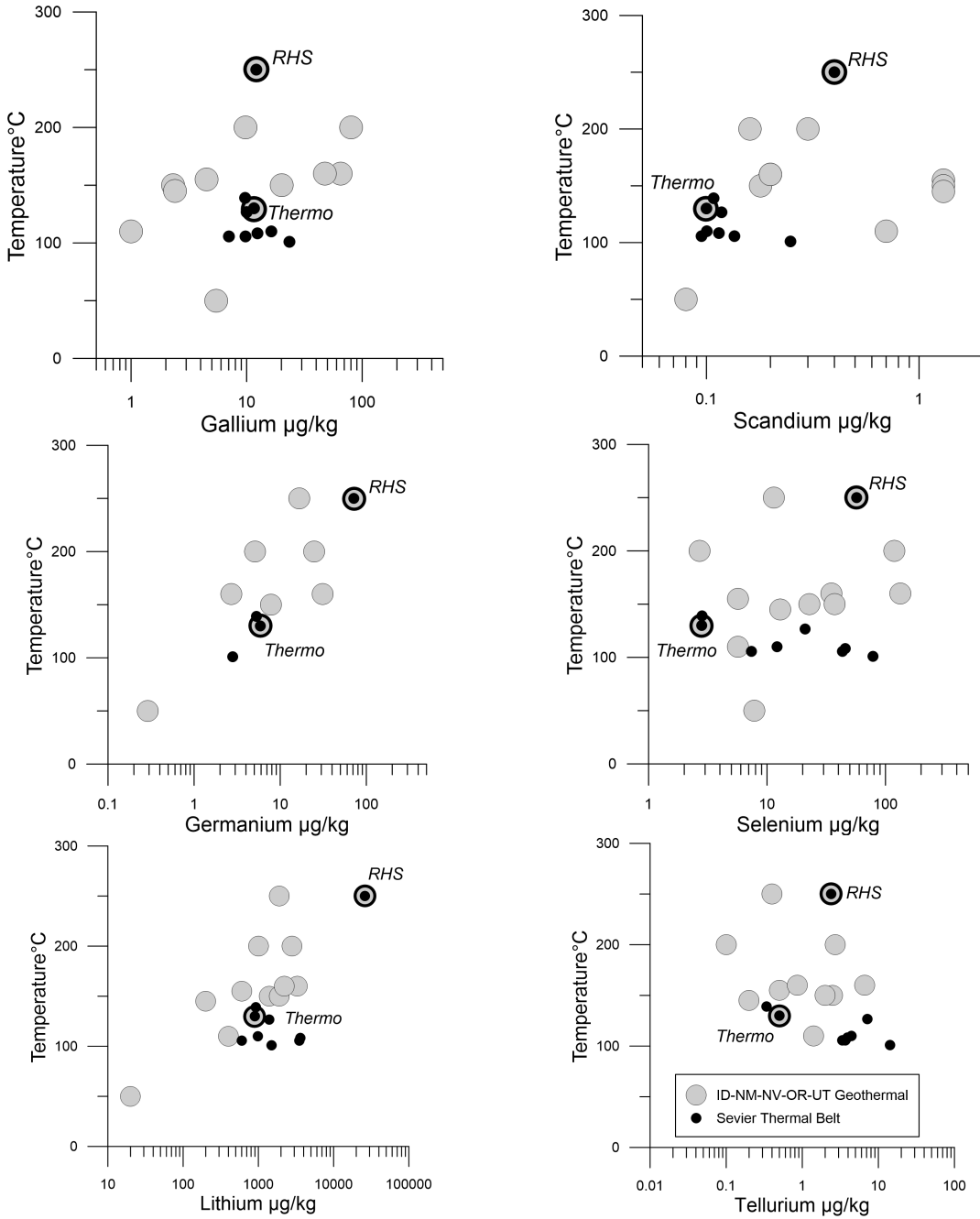


Figure 24. Concentrations ( $\mu\text{g}/\text{kg}$  or ppb) of gallium, germanium, lithium, scandium, selenium, and tellurium in Sevier Thermal Belt and produced geothermal waters plotted against measured temperatures (Table 2). Roosevelt Hot Springs (RHS) and Thermo samples are denoted by the black-filled circles, which are surrounded by larger grey-filled circles and bold black outlines.

This report is written for public disclosure.

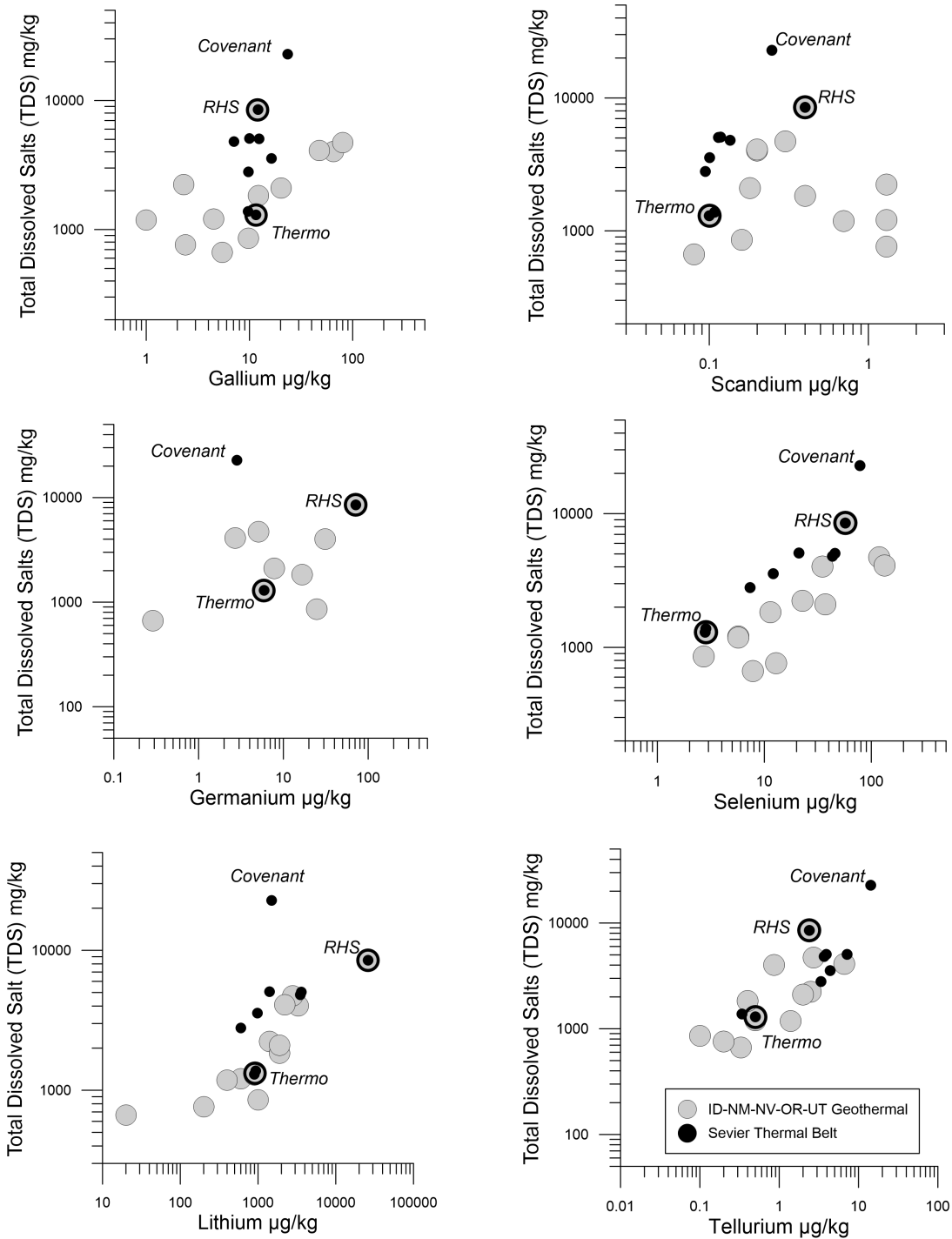


Figure 25. Concentrations ( $\mu\text{g}/\text{kg}$  or ppb) of gallium, germanium, lithium, scandium, selenium, and tellurium in Sevier Thermal Belt and produced geothermal waters plotted against total dissolved salts ( $\text{mg}/\text{kg}$  or ppm; Table 2). The most saline water is from the Covenant oil field. Roosevelt Hot Springs (RHS) and Thermo samples are denoted by the black-filled circles, which are surrounded by larger grey-filled circles and bold black outlines.

This report is written for public disclosure.

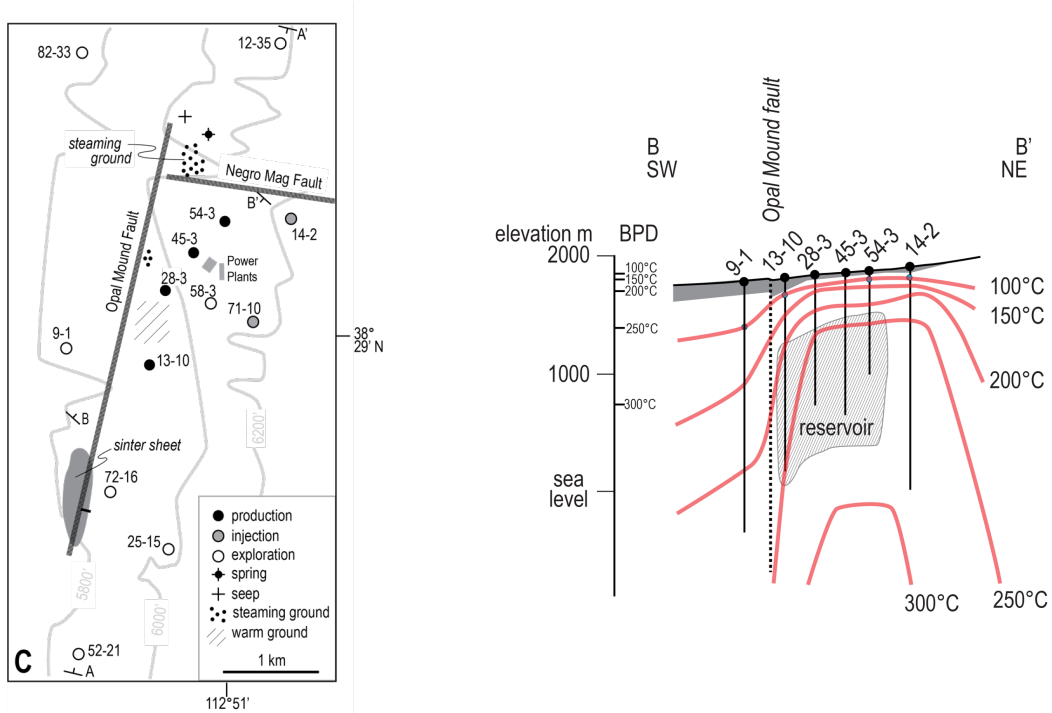


Figure 26. Sketch production field map and cross section of Roosevelt Hot Springs, showing the native state thermal structure (Faulder, 1994; Glenn and Hulen, 1979; Glenn et al., 1980; Allis et al., 2016). The host lithology for most of the system is made of Miocene granitic rock (white), which is capped by a thin veneer of alluvium (medium grey). For simplicity, the Opal Mound fault is shown as having vertical dip, although it likely dips steeply eastward (Nielson et al., 1986). The hydrostatic boiling point for depth temperature gradient (BPD) is referenced to a piezometric level over the hot upflow between wells 54-2 and 14-2. The shaded region denoted reservoir refers to the zone of geothermal energy exploitation tapped by deep wells.

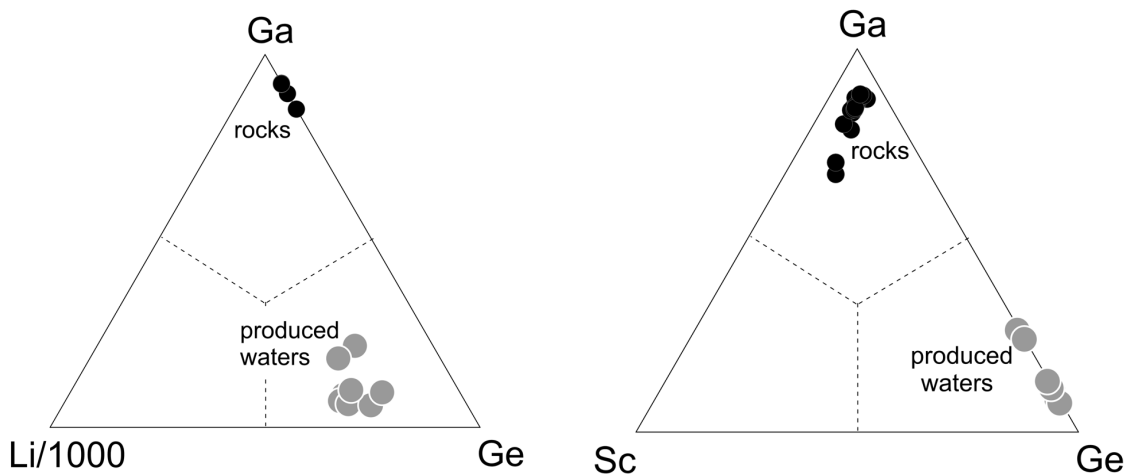


Figure 27. Relative concentrations of gallium, germanium, lithium and scandium in granitic rocks of the Mineral Mountains and produced waters from Roosevelt Hot Springs.

This report is written for public disclosure.

Gallium, germanium, lithium, scandium, selenium and tellurium concentrations in produced geothermal waters are compared to Sevier Thermal Belt waters as a function of TDS (Fig. 25). Selenium and tellurium show the strongest correlations with TDS, with the highest concentrations being found in the most saline water from Covenant oil field. If the Covenant oil field water is omitted, then in all other thermal waters, lithium shows a strong correlation with TDS. For gallium and germanium, correlations with TDS are weak to modest. These trends imply that TDS values influence the concentrations of lithium, selenium, and tellurium in thermal waters, and much less so for gallium, germanium, and scandium.

Of the producing fields studied, Roosevelt Hot Springs is one of the more important in terms of the concentrations and inventories of SCVM, including germanium and lithium. The field occurs at the base of the Mineral Mountains, and the reservoir is entirely hosted in granitic rocks (Capuano and Cole, 1982; Nielson et al., 1986) and the preproduction reservoir temperature was 265°C (Fig. 26). The field commenced production in 1984, and over time the production fluids have undergone considerable enrichment in aqueous TDS due to effects of mixing with flashed injectate (Simmons et al., 2018). To see if there might be a lithologic control, the relative concentrations of gallium, germanium, lithium and scandium in produced waters and reservoir rocks are compared using trilinear plots (Fig. 27). The clear separation of rock and produced water data into distinct clusters implies that SCVM concentrations in produced waters are being influenced by a range of processes, over and above effects which can be attributed to simple transfer of elements by hydrothermal water-rock interaction and mineral dissolution, but TDS concentrations might be particularly important in enhancing the lithium concentration.

#### *Helium in the North Milford Valley*

Roosevelt Hot Springs and the Utah FORGE EGS site are located in the North Milford Valley, and in the course of this work a large helium anomaly associated with shallow groundwaters that extends beyond the production field of Roosevelt Hot Springs was identified (Figs. 20 and 28). The average helium concentration in shallow groundwaters is 2.6E-06 ccSTP/g and the average R/Ra value is 2.1, and these values are similar to those measured in Roosevelt Hot Springs production waters (Table 2, Tab-North Milford Valley). Assuming a groundwater reservoir volume of 30 km<sup>3</sup>, the calculated inventory of helium is about 2 million kg similar to calculated inventories for Raft River and Patua (Fig. 15); the inventory of <sup>3</sup>He is about 4.5 kg. The R/Ra values indicate the non-thermal groundwater helium has a mantle component. Furthermore, the oxygen and hydrogen isotope and the Cl-HCO<sub>3</sub>-SO<sub>4</sub> data (Fig. 28) show considerable variation, which cannot be explained by a single water source or a simple mixing trend. From this, it appears that deep-seated helium has been incorporated (via diffusion?) into shallow groundwaters that are compositionally heterogeneous.

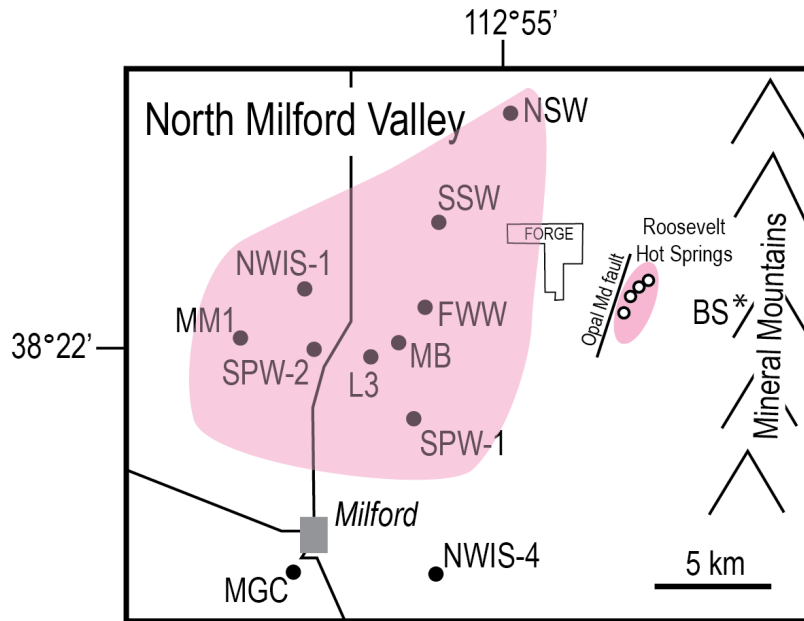


Figure 28. Sketch map of the North Milford Valley in southwestern Utah, showing the locations of Roosevelt Hot Springs, the Utah FORGE EGS site, and shallow groundwater wells north of Milford. The pink filled areas outline the zones with helium compositions with R/Ra values around 2.1.

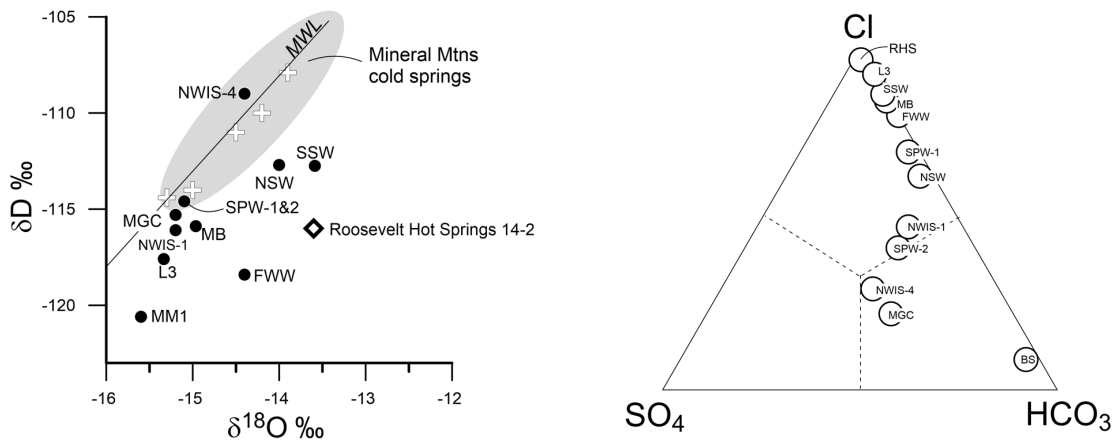


Figure 29: Stable isotope compositions and Cl-HCO<sub>3</sub>-SO<sub>4</sub> graph showing the compositional variability of shallow groundwaters in the North Milford Valley.

This report is written for public disclosure.

## COMPARISONS WITH SCVM MINERAL DEPOSITS

Table 5 summarizes the geological settings and characteristics of SCVM deposits. It shows that SCVM may be recovered either as primary commodities or as by-products from mining of other commodities. For example, nearly 90% of the world production of niobium is from the Araxá niobium mine (Brazil), whereas gallium is recovered primarily as a byproduct commodity of bauxite mining or as a byproduct of zinc processing from a number of sources worldwide. Niobium, gallium and tellurium are associated with well documented deposit types, but many of the other SCVM are not so easily characterized. The geologic and geochemical processes that lead to ore-grade enrichment for a number of SCVM are summarized by Gunn (2014), Verplanck and Hitzman (2016), and Schultz et al. (2017).

### *SCVM Mineral Deposits in the Basin and Range*

The known deposit types with potential for SCVM in the Basin and Range include: (1) porphyry Cu (and associated polymetallic veins), (2) epithermal, (3) volcanogenic massive sulfide (VMS), (4) skarn, (5) small magmatic Ni-Cu, (6) tin-bearing rhyolite commonly associated with porphyry Mo deposits, (7) solution collapse breccias (Kipushi?), (8) heavy mineral sand deposits, and (9) small REE-bearing (allanite) intrusive centers. Specific commodity information and trace element contents of mineral deposits and occurrences are taken from <https://mrdata.usgs.gov/mrds/find-mrds.php>.

Gallium (average grade of 0.0419 wt. % or 419,000 ug/kg) and germanium (0.115 wt. % or 1,115,000 ug/kg) were historically considered primary products (along with Cu, Pb, and Ag) of mining from solution collapse breccias in marine carbonate rocks at the Dixie and Apex mines. These are located in southwestern Utah about 140 km southwest of the Thermo hot springs site of this study, but Mississippian-Pennsylvanian limestone located elsewhere are prospective host rocks. Tin-bearing rhyolite porphyry/breccia occurrences (Tetons Breccia about 30 km west of Thermo hot springs and the Gallium prospect located ~70 km southwest of the Roosevelt hot springs site) reportedly also contain elevated concentrations of gallium and niobium.

Although never historically produced, high average concentrations of tellurium of ~4.8 mg/kg (Table 5) are reported in the Bingham porphyry deposit (Utah), and the tellurium-bearing ore minerals volynskite and hedleyite, although very rare worldwide, are relatively common in the Fortitude and Copper Canyon skarn deposits (Nevada). One vein deposit in shale (Telluride deposit) near the Fortitude and Copper Canyon deposits contains tetradymite. The skarn and tetradymite localities are about 45 km west of the Beowawe geothermal field. Other deposits considered to have potential for high tellurium are epithermal veins such as the Sleeper deposit in northern Nevada, about 35 km north northeast of the Blue Mountain, and the Buster mine 30 km west of the Patua. Carlin-type deposits with high reported tellurium contents include Getchell (as much as 180 mg/kg) and smaller associated deposits located about 75 km northeast of Blue Mountain.

Cobalt concentrations are high in some skarn deposits (Fortitude and Copper Canyon deposits 45 km west of Beowawe), the VMS Big Mike deposit ~60 km northeast of Dixie Valley, and in particular in small gabbro-hosted nickel-cobalt deposits such as Cottonwood Canyon, Bell, and

This report is written for public disclosure.

Lovelock deposits located about 7 km southwest of the Dixie Valley. Similar to that reported for tellurium, epithermal vein deposits such as Sleeper also reportedly contain high cobalt.

Elevated concentrations of selenium occur in the Bingham porphyry Cu deposit (high grade ore averages 12 mg/kg), and in the Mule Canyon epithermal Au-Ag deposit located 8 km west of the Beowawe. Epithermal veins at the Rosebud and Lantern prospects, ~50 km southwest of Blue Mountain, the Sleeper deposit to the north, and the Hazel and Green epithermal deposits about 75 km west of Dixie Valley and 40 km northeast of Patua location all contain elevated selenium too as indicated by the presence of naumannite, a silver selenide mineral, in these deposits.

Anomalously high REE-niobium concentrations are reported at the Sheeprock deposit ~200 km west of the Uinta Basin, and allanite, a REE silicate mineral, at the Red Rock prospect in western Nevada about 95 km west of Soda Lake, which is likely associated with alkaline intrusive rocks, although information is limited. Heavy mineral sands near Lake Bonneville in Utah, as well as scattered occurrences in western and southern Nevada, contain monazite, sphene, and zircon.

#### *Comparison with SCVM in Produced Waters*

From the analyses of produced waters (Table 2, Figs. 10 and 11), the most relevant insights from the geological compilation of SCVM metal deposit types (Table 5) relate to gallium, germanium, lithium, scandium, selenium, and tellurium. Niobium, platinum group elements (PGE), REE, and rhenium are generally associated with igneous intrusions and high temperature hydrothermal environments (>300° C). Produced thermal waters generally contain low REE concentrations (<5 ug/kg) because these elements are highly insoluble in neutral pH waters (e.g., Neupane and Wendt, 2017; Smith et al., 2017).

Gallium and germanium are recovered from Mississippi Valley-Type base-metal deposits, which form at <200° C from basinal brines, which is consistent with the high concentrations found in Uinta basin waters compared to geothermal waters (Figs. 10 and 11).

Lithium is recovered from brines produced from lacustrine evaporite deposits (also called salars in Latin America) and from spodumene, a Li-rich feldspar occurring in pegmatites. Of all the SCVM elements evaluated in this study, lithium is the most concentrated metal in produced waters, with Roosevelt Hot Springs having the highest measured concentration (20-30 mg/kg) and the largest calculated inventory (7 million kg; Figs. 10, 11 and 12). For comparison, lithium concentrations in the highly saline brines produced from the Salton Sea range from 100 to 400 mg/kg (McKibben and Hardie, 1997; Kesler et al., 2012; Neupane and Wendt, 2017); the Salton Sea has a total estimated lithium resource of about 300,000 t (3,000,000,000 kg), which is 40 times larger than the estimated lithium resource for Roosevelt Hot Springs (Fig. 12).

Scandium is a by-product of mining REEs (iron and uranium) from a small number of deposits in China and Russia, with 90% of the global production coming from Bayan Obo in China (Williams-Jones and Vasyukova, 2018), and scandium production in the USA is sparse (US Geological Survey Mineral Commodity Summary, 2012). The geochemical behavior of scandium in hydrothermal waters is poorly studied, but it likely forms hydroxyl complexes (Williams-Jones and Vasyukova, 2018). Produced geothermal waters contain between 0.1 and 2

This report is written for public disclosure.

ug/kg Sc, but the Paradox Basin produced waters contain up to 10 ug/kg Sc, suggesting that high TDS helps to mobilize this element (Figs. 10 and 11).

Selenium and tellurium are commonly found in association with epithermal gold-silver deposits, which form at temperatures of 200-250° C from dilute near neutral pH solutions. The produced waters from geothermal fields are similar in chemistry to solutions producing epithermal mineralization, but the concentrations of both elements are relatively low in comparison to the concentrations found in the Uinta Basin waters (Figs. 10 and 11). For comparison, tellurium concentrations in produced waters from New Zealand geothermal fields are up to 2000 ug/kg (Simmons et al., 2016b). The analysis of Dixie Valley calcite scales (28-33A, Table 3) contains significant selenium (14 mg/kg) and tellurium (4 mg/kg) suggesting that these elements might be depositing in geothermal wells and pipelines due to boiling.

### **CONSIDERATIONS FOR FUTURE WORK**

The data reported in this project are preliminary in nature. With the resources available, effort was directed at evaluating the potential ranges of SCVM in produced fluids from a large number of fields in different geologic settings across the Basin and Range province. Thus, many samples have been analyzed for a wide range of SCVM, which represent a diverse group of trace elements with wide ranging chemical characteristics.

While the laboratory analyses of SCVM were checked against standards, the large range of fluid compositions means that matrix effects could affect the accuracy of the analytical results. To improve the level of confidence, repeat analyses of several fluid samples acquired from the same well over a period of a few months should be analyzed in conjunction with aqueous standards whose matrix has been adjusted to match the sample fluid composition. To check for geospatial variability, samples need to be analyzed from all production wells within a single field. Based on the results, the most promising geothermal candidates for more detailed study include Dixie Valley, Patua, Raft River, Roosevelt Hot Springs, and Soda Lake.

The Uinta and Paradox Basins fluids also require more detailed study as samples were acquired from widely spaced wells that tap various parts of large geologically complex oil and gas reservoirs. The high salinities in the Paradox Basin fluids required significant dilution prior to analysis, which raised analytical detection limits. These are surmountable problems, and the main thing to appreciate is that high quality analyses will require extra time and effort by analysts doing the work.

Mineral recovery and commercial viability assessment were beyond the scope of this study. Nonetheless, the relatively low concentrations of SCVM measured in produced waters implies that extraction technologies will need to be very efficient to be effective. Until these technologies are proven, mineral recovery research will dominate the focus of efforts to extract SCVM from produced waters.

**Acknowledgment:** This material is based upon work supported by the Department of Energy under Award Number DE-EE0007604.

This report is written for public disclosure.

**Disclaimer:** This report was prepared as an account of work sponsored by an agency of the United States Government. Neither the United States Government nor any agency thereof, nor any of their employees, makes any warranty, express or implied, or assumes any legal liability or responsibility for the accuracy, completeness, or usefulness of any information, apparatus, product, or process disclosed, or represents that its use would not infringe privately owned rights. Reference herein to any specific commercial product, process, or service by trade name, trademark, manufacturer, or otherwise does not necessarily constitute or imply its endorsement, recommendation, or favoring by the United States Government or any agency thereof. The views and opinions of authors expressed herein do not necessarily state or reflect those of the United States Government or any agency thereof.

## References

Allis, R., Moore, J., Gwynn, M., Kirby, S., and Sprinkel, D., 2011, The potential for basin-centered geothermal resources in the Great Basin. *GRC Transactions*, v. 35, p. 683-688.

Allis, R.G., Hardwick, C., Gwynn, M., and Johnson, S., 2015, Pavant Butte, Utah geothermal prospect revisited: *Geothermal Resources Council Transactions*, 39, 379-387.

Allis, R.G., Moore, J.N., Davatzes, N., Gwynn, M., Hardwick, C., Kirby, S., Pankow, K., Potter, S., and Simmons, S.F., 2016. EGS Concept Testing and Development at the Milford, Utah FORGE Site: Proceedings, 41<sup>st</sup> Workshop on Geothermal Reservoir Engineering, Stanford University, Stanford, CA.

Allis, R.G., Gwynn, M., Hardwick, C., Kirby, S., Bowers, R., Moore, J., Wannamaker, P., and Simmons, S., 2017, Characteristics of the Cove Fort-Dog Valley-Twin Peaks thermal anomaly, Utah: Proceedings, 42nd Workshop on Geothermal Reservoir Engineering, Stanford University, Stanford, CA.

Allis, R.G., Gwynn, M., Hardwick, C., Hurlbut, W., and Moore, J., 2018, Thermal characteristics of the FORGE site, Milford, Utah: *Geothermal Resources Council Transactions*, v. 42, p. 15.

Benato, S., Hickman, S., Davatzes, N.C., Taron, J., Spielman, P., Elsworth, D., Majer, E. L., and Boyle, K., 2016, Conceptual model and numerical analysis of the Desert Peak EGS project: Reservoir response to the shallow medium flow-rate hydraulic stimulation phase: *Geothermics*, v. 63, p. 139-156.

Benoit, D., and Butler, R.W., 1983, A review of high-temperature geothermal developments in the northern Basin and Range province: *Geothermal Resources Council Special Report 13*, p. 57-80.

Blackwell, D.D., Richards, M.C., Frone, Z.S., Batir, J.F., Williams, M.A., Ruzo, A.A., and Dingwall, R.K., 2011, SMU Geothermal Laboratory Heat Flow Map of the Co-terminous United States, <http://www.smu.edu/geothermal>.

This report is written for public disclosure.

Bradford, J., McLennan, J., Moore, J., Podgorney, R., Nash, G., Mann, M., Rickard, W., and Glaspey, D., 2016, Numerical modeling of the stimulation program at RRG-9 ST1: Proceedings 41st Workshop on Geothermal Reservoir Engineering, Stanford University, Stanford, CA.

Blackett, R. E., and Wakefield, S.I., 2002, Geothermal resources of Utah, a digital atlas of Utah's geothermal resources. Utah Geological Survey, OFR-397, CD-ROM.

Coolbaugh, M., Zehner, R., Kreemer, C., Blackwell, D., Oppliger, G., Sawatzky, D., Blewitt, G., Pancha, A., Richards, M., Helm-Clark, C., Shevenell, L., Raines, G., Johnson, G., Minor, T., and Boyd, T., 2005, Geothermal potential map of the Great Basin region, western United States: Nevada Bureau of Mines and Geology, Map 151, 1 Plate.

Capuano, R. M., and Cole, D. R., 1982, Fluid-mineral equilibria in a hydrothermal system. *Geochimica Cosmochimica Acta*, v. 46, p. 1353-1364.

Craig, H., 1961 Isotopic variations in meteoric water, *Science*, v. 133, p. 1702-1703.

Craig, H. 1963, The isotope geochemistry of water and carbon in geothermal areas. *Nuclear Geology of Geothermal Areas*, Spoleto, Italy, Consiglio Nazionale Ricerche, Pisa, p. 17-53.

Dickinson, W.R., 2006, Geotectonic evolution of the Great Basin: *Geosphere*, v. 2, p. 353-368.

Eaton, G.P., 1982, The Basin and Range Province: Origin and Tectonic Significance: *Annual Reviews Earth and Planetary Sciences*, v. 10, p. 409-440.

Elders, W.A. and Moore, J.N., 2016, Geology of geothermal resources: in *Geothermal Power Generation Developments and Innovation* (ed. R. DiPippo), Woodhead Publishing Series in Energy: Number 97, Elsevier, p. 7-32.

Faulder, D.D., 1994, Long-term flow test #1, Roosevelt Hot Springs, Utah. *Transactions, Geothermal Resources Council Transactions*, 18, 583-590.

Faulds, J.E., and Hinz, N., 2015, Favorable Tectonic and Structural Settings of Geothermal Systems in the Great Basin Region, Western USA: Proxies for Discovering Blind Geothermal Systems: *Proceedings, World Geothermal Congress 2015*, Melbourne, Australia.

Flynn, T. and Buchanan, P.L., 1990, Pleistocene origin of geothermal fluids in the Great Basin, western United States: *Resource Geology Special Issue*, **16**, p. 60-68.

Fournier, R. O., 1991, Water geothermometers applied to geothermal energy. *Applications of Geochemistry in Geothermal Reservoir Development*, UNITAR-UNDP, p. 37-69.

Giggenbach, W. F., 1988, Geothermal solute equilibria. Derivation of Na-K-Mg-Ca geoinidicators. *Geochimica Cosmochimica Acta*, v. 52, p. 2749-2765.

This report is written for public disclosure.

Glenn, W.E., and Hulen, J. B., 1979, Interpretation of well log data from four drill holes at Roosevelt Hot Springs KGRA. DOE Earth Science Laboratory Report, University of Utah, pp. 74.

Gunn, G., ed., 2014, *Critical Metals Handbook*, John Wiley & Sons, Oxford. 439 p.  
National Research Council, 2008, *Minerals, critical minerals, and the U.S. Economy: The National Academy Press*, Washington, D.C., 264 p.

Gwynn, M., Allis, R., and Kirby, S., 2018, Shallow thermal anomalies and the deep thermal regime in west-central Utah: Utah Geological Association Guidebook Publication, v. 47, p. 119-137.

Hintze, L.F., and Davis, F.H., 2003, *Geology of Millard County, Utah: Utah Geological Survey Bulletin 133*, 305 p.

Hintze, L.F., Willis, G.C., Laes, Y.M., Sprinkel, D.A., and Brown, K.D., 2000, Digital geologic map of Utah: Utah Geological Survey Map 179DM, scale 1:500,000.

Kesler, S.E., Gruber, P.W., Medina, P. A., Keoleian, G. A., Everson, M.P., and Wallington, T.J., 2012, Global lithium resources: Relative importance of pegmatite, brine, and other deposits: *Ore Geology Reviews*, v. 48, p. 55-69.

Kirby, S., 2012, Geologic and hydrologic characterization of regional nongeothermal groundwater resources in the Cove Fort area, Millard and Beaver Counties, Utah, Utah Geological Survey Special Study 140, p. 65.

Lachenbruch, A.H., and Sass, J.H., 1978, Models of extending lithosphere and heat flow in the Basin and Range province: *Geological Society of America Memoir 152*, p. 209-250.

Moore, J., McLennan, J., Allis, R., Pankow, K., Simmons, S., Podgorney, R., Wannamaker, P., Bartley, J., Jones, C., and Rickard, W., 2019, *The Utah Frontier Observatory for Research in Geothermal Energy (FORGE): An International Laboratory for Enhanced Geothermal System Technology Development: Proceedings 43rd Workshop on Geothermal Reservoir Engineering*, Stanford University, Stanford, CA.

Mabey, D.R., and Budding, K.E., 1987, High temperature geothermal resources of Utah. Utah Geological and Mineralogical Survey, Bulletin 123, 64 pp.

McKibben, M.A., and Hardie, L.A., 1997, Ore-forming brines in active continental rifts: *Geochemistry of Hydrothermal Ore Deposits (3<sup>rd</sup> ed)*, Editor H.L. Barnes, John Wiley & Sons, p. 877-935.

Nielson, D. L., Evans, S.H., and Sibbett, B.S., 1986, Magmatic, structural, and hydrothermal evolution of the Mineral Mountains intrusive complex, Utah. *Geological Society of America Bulletin*, v. 97, p. 765-777.

This report is written for public disclosure.

Neupane, G. and Wendt, D.S, 2017, Assessment of mineral resources in geothermal brines in the USA. Proceedings 42nd Workshop Geothermal Reservoir Engineering, Stanford University, Stanford, CA, USA.

Parry, W.T., Chan, M. A., and Nash, B.P., 2009, Diagenetic characteristics of the Jurassic Navajo sandstone in the Covenant oil field, central Utah thrust belt: AAPG Bulletin, v. 93, p. 1039-1061.

Person, M., Banerjee, A., Hofstra, A., Sweetkind, D., and Gao, Y., 2008, Hydrologic models of modern and fossil geothermal systems in the Great Basin: Genetic implications for epithermal Au-Ag and Carlin-type gold deposits: Geosphere, v.4, p. 888–917.

Ross, H.P., Blackett, R.E., Shubat, M. A., and Gloyn, R. W., 1991, Self-potential and fluid chemistry studies of the Meadow-Hatton and Abraham hot springs, Utah. Geothermal Resources Council Transactions, v. 17, p. 167-174.

Ryan, W.B.F., S.M. Carbotte, J.O. Coplan, S. O'Hara, A. Melkonian, R. Arko, R.A. Weissel, V. Ferrini, A. Goodwillie, F. Nitsche, J. Bonczkowski, and R. Zemsky, 2009, Global Multi-Resolution Topography synthesis: Geochem. Geophys. Geosyst., 10, Q03014, doi:[10.1029/2008GC002332](https://doi.org/10.1029/2008GC002332).

Schultz, K.J., DeYoung, J.H. Jr., Seal, R.R. II, and Bradley, D.C., eds., 2017 Critical mineral resources of the United States – Economic and environmental geology and prospects for future supply: U.S. Geological Survey Professional Paper 1802.

Seward, T.M., and Barnes, H.L., 1997, Metal transport by hydrothermal ore fluids: Geochemistry of hydrothermal ore deposits, 3rd ed.: John Wiley and Sons, p. 435–486.

Siler, D. L., and Kennedy, B.M., 2016, Regional crustal-scale structures as conduits for deep geothermal upflow: Geothermics, 59, p. 27-37.

Simmons, S.F., Kirby, S., Moore, J.N., Wannamaker, P., and Allis, R., 2015, Comparative analysis of fluid chemistry from Cove Fort, Roosevelt and Thermo: Implications for geothermal resources and hydrothermal systems on the east edge of the Great Basin. Geothermal Resources Council Transactions, 39, 55-61.

Simmons, S. F., Kirby, S., Jones, C., Moore, J., and Allis, R., 2016a, The Geology, Geochemistry, and Hydrology of the EGS FORGE Site, Milford Utah. Proceedings, 41st Workshop on Geothermal Reservoir Engineering, Stanford University, Stanford, CA, p. 1181-1190.

Simmons, S. F., Brown, K. L., and Tutulo, B. M., 2016b, Hydrothermal transport of Ag, Au, Cu, Pb, Te, Zn, and other metals and metalloids in New Zealand geothermal systems: Spatial

This report is written for public disclosure.

Patterns, Fluid-mineral Equilibria, and Implications for Epithermal Mineralization: *Economic Geology*, p. 589-618.

Simmons, S.F., Kirby, S., Allis, R., Moore, J.N., and Fischer, T., 2018, Update on the production chemistry of Roosevelt Hot Springs reservoir: Proceedings, 43rd Workshop on Geothermal Reservoir Engineering, Stanford University, Stanford, CA.

Simmons, S.F., Kirby, S., Allis, R., Wannamaker, P., and Moore, J.N., 2019, Geothermal Resources and Hydrothermal Activity in the Sevier Thermal Belt Based on Fluid Geochemistry: Proceedings, 43rd Workshop on Geothermal Reservoir Engineering, Stanford University, Stanford, CA.

Smith, Y.R., Kumar, P., and McLennan, J.D., 2017, On the extraction of rare earth elements from geothermal brines: *Resources*, v. 6, 16 p.

Sorey, M., Nathenson, M., and Smith, C., 1982, Methods for assessing low-temperature geothermal resources: U. S. Geological Survey Circular 892, p. 17-30.

Taylor, H.P., 1997, Oxygen and hydrogen isotope relationships in hydrothermal mineral deposits. *Geochemistry of Hydrothermal Ore Deposits*, 3rd edition: John Wiley & Sons, Inc, p. 229-302.

Verplanck, P.L., and Hitzman, M.W., 2016, Rare earth and critical elements in ore deposits: *Reviews in Economic Geology*, v. 18, 350 p.

Wannamaker, P. E. , Bartley, J. M. , Sheehan, A. F., Jones, C. H., Lowry, A. R. , Dumitru, T. A., Ehlers, T. A., Holbrook, W. S. Farmer, G. L., Unsworth, M. J. , Hall, D. B. , Chapman, D. S., Okaya, D. A., John, B. E., and Wolfe, J. A., 2001, Great Basin-Colorado Plateau transition in central Utah: An interface between active extension and stable interior: in *The Geological Transition: Colorado Plateau to Basin and Range*, (eds. M. C. Erskine, J. E. Faulds, J. M. Bartley and P. Rowley), UGA/AAPG Guidebook 30/GB78, p. 1-38.

Wannamaker, P. E., Hasterok, D. P., Johnston, J. M., Stodt, J. A., Hall, D. B., Sodergren, T. L., Pellerin, L., Maris, V., Doerner, W. M., and Unsworth, M. J., 2008, Lithospheric dismemberment and magmatic processes of the Great Basin-Colorado Plateau transition, Utah, implied from magnetotellurics: *Geochemistry, Geophysics, Geosystems*, 9, Q05019, doi:10.1029/2007GC001886.

Wannamaker, P. E., Pankow, K. L., Moore, J. N., Nash, G. D., Maris, V., Simmons, S.F., and Hardwick, C. L., 2016, A Play Fairway Analysis for Structurally Controlled Geothermal Systems in the Eastern Great Basin Extensional Regime, Utah. Proceedings 41<sup>st</sup> Workshop on Geothermal Reservoir Engineering, Stanford University, Stanford, CA.

Williams-Jones, A.E. and Vasyukova, O.V., 2018, The economic geology of scandium, the runt of the rare earth litter: *Economic Geology*, v. 113, p. 973-988.

This report is written for public disclosure.

Williams, C.F., M.J. Reed, R.H. Mariner, J. DeAngelo, and S.P. Galanis Jr., 2008, Assessment of moderate- and high-temperature geothermal resources of the United States: USGS Fact Sheet 2008-3082, <http://pubs.usgs.gov/fs/2008/3082/>

This report is written for public disclosure.